

ผลของการเติมทั้งสแตนลงบนตัวเร่งปฏิกิริยา NiMo/Al<sub>2</sub>O<sub>3</sub> และ CoMo/Al<sub>2</sub>O<sub>3</sub> สำหรับกระบวนการ  
ไฮโดรโพรเซสซิงในการผลิตไบโอดีเซล

นายพงศธร จันทรักษ์

วิทยานิพนธ์นี้เป็นส่วนหนึ่งของการศึกษาตามหลักสูตรปริญญาวิศวกรรมศาสตรมหาบัณฑิต

สาขาวิชาวิศวกรรมเคมี ภาควิชาวิศวกรรมเคมี

คณะวิศวกรรมศาสตร์ จุฬาลงกรณ์มหาวิทยาลัย

ปีการศึกษา 2555

ลิขสิทธิ์ของจุฬาลงกรณ์มหาวิทยาลัย

บทคัดย่อและแฟ้มข้อมูลฉบับเต็มของวิทยานิพนธ์ตั้งแต่ปีการศึกษา 2554 ที่ให้บริการในคลังปัญญาจุฬาฯ (CUIR)

เป็นแฟ้มข้อมูลของนิสิตเจ้าของวิทยานิพนธ์ที่ส่งผ่านทางบัณฑิตวิทยาลัย

The abstract and full text of theses from the academic year 2011 in Chulalongkorn University Intellectual Repository (CUIR) are the thesis authors' files submitted through the Graduate School.

EFFECT OF TUNGSTEN LOADING ON NiMo/Al<sub>2</sub>O<sub>3</sub> AND CoMo/Al<sub>2</sub>O<sub>3</sub>  
CATALYSTS FOR HYDROPROCESSING OF BIODIESEL PRODUCTION

Mr. Pongsatorn Jantharak

A Thesis Submitted in Partial Fulfillment of the Requirements  
for the Degree of Master of Engineering Program in Chemical Engineering

Department of Chemical Engineering

Faculty of Engineering

Chulalongkorn University

Academic Year 2012

Copyright of Chulalongkorn University

Thesis Title           EFFECT OF TUNGSTEN LOADING ON NiMo/Al<sub>2</sub>O<sub>3</sub> AND  
CoMo/Al<sub>2</sub>O<sub>3</sub> CATALYSTS FOR HYDROPROCESSING OF  
BIODIESEL PRODUCTION  
By                       Mr. Pongsatorn Jantharak  
Field of Study        Chemical Engineering  
Thesis Advisor       Professor Suttichai Assabumrungrat, Ph.D.  
Thesis Co-advisor   Assistant Professor Worapon Kiatkittipong, D.Eng.

---

Accepted by the Faculty of Engineering, Chulalongkorn University in Partial  
Fulfillment of the Requirements for the Master's Degree

.....Dean of the Faculty of Engineering  
(Associate Professor Boonsom Lerthirunwong, Dr.Eng.)

#### THESIS COMMITTEE

.....Chairman  
(Assistant Professor Anongnat Somwangthanaroj , Ph.D.)

.....Thesis Advisor  
(Professor Suttichai Assabumrungrat, Ph.D.)

.....Thesis Co-advisor  
(Assistant Professor Worapon Kiatkittipong, D.Eng.)

.....Examiner  
(Assistant Professor Suphot Phatanasri, D.Eng.)

.....External Examiner  
(Associate Professor Navadol Laosiripojana, Ph.D.)

พงศธร จันทรักษ์ : ผลของการเติมทั้งสแตนลงบนตัวเร่งปฏิกิริยา NiMo/Al<sub>2</sub>O<sub>3</sub> และ CoMo/Al<sub>2</sub>O<sub>3</sub> สำหรับกระบวนการไฮโดรโพรเซสซิงในการผลิตไบโอดีเซล (EFFECT OF TUNGSTEN LOADING ON NiMo/Al<sub>2</sub>O<sub>3</sub> AND CoMo/Al<sub>2</sub>O<sub>3</sub> CATALYSTS FOR HYDROPROCESSING OF BIODIESEL PRODUCTION) อ. ที่ปรึกษาวิทยานิพนธ์หลัก: ศ.ดร. สุทธิชัย อัสสะบารุงรัตน์ , อ. ที่ปรึกษาวิทยานิพนธ์ร่วม: ผศ.ดร.วรพล เกียรติกิตติพงษ์, 71 หน้า.

งานวิจัยนี้ศึกษาผลของการเติมทั้งสแตนลงบนตัวเร่งปฏิกิริยา NiMo/Al<sub>2</sub>O<sub>3</sub> และ CoMo/Al<sub>2</sub>O<sub>3</sub> ที่ใช้สำหรับการผลิตไบโอดีเซลด้วยกระบวนการไฮโดรโพรเซสซิง สภาวะที่ใช้ดำเนินการคืออุณหภูมิ 300-400 องศาเซลเซียส ความดันของไฮโดรเจน 40 บาร์ และเวลาในการทำปฏิกิริยา 1-4 ชั่วโมง โดยใช้ตัวเร่งปฏิกิริยาคาร์ไบด์เคชันของ นิกเกิล โมลิบดีนัม และ โคบอลต์ โมลิบดีนัม ซึ่งมีการเติมและไม่เติม ทั้งสแตน บนตัวรองรับอะลูมินา นอกจากนี้กรดไขมัน 3 ชนิด ประกอบด้วย กรดโอเลอิก กรดสเตียริก และกรดปาล์มมิก ถูกใช้เป็นสารตั้งต้น พบว่าผลิตภัณฑ์ที่เกิดจากปฏิกิริยา โอลิโกเมอร์ไรเซชัน จะพบที่อุณหภูมิต่ำกว่า 350 องศาเซลเซียส ที่ระยะเวลาในการทำปฏิกิริยาในช่วงสั้นๆ ในขณะที่ผลิตภัณฑ์ที่เกิดจากการแครกกิง จะเกิดที่อุณหภูมิสูงและหรือที่ระยะเวลาในการทำปฏิกิริยาที่นาน โดยร้อยละผลได้ของดีเซลสูงสุด อยู่ที่ 66.9 จากการทดลองกระบวนการไฮโดรโพรเซสซิงของกรดโอเลอิก โดยใช้ตัวเร่งปฏิกิริยานิกเกิล โมลิบดีนัมที่เติมทั้งสแตน ที่ดำเนินการที่อุณหภูมิ 350 องศาเซลเซียส เวลาทำปฏิกิริยา 2 ชั่วโมง และความดันไฮโดรเจน 40 บาร์ ผลิตภัณฑ์ของเหลวที่ได้คือไฮโดรคาร์บอนที่มีคาร์บอนอะตอมอยู่ในช่วง 15-18 อะตอม และน้ำ ในขณะที่ผลิตภัณฑ์แก๊สที่ได้ ประกอบไปด้วย คาร์บอนมอนอกไซด์ คาร์บอนไดออกไซด์ และมีเทน

ภาควิชา ..... วิศวกรรมเคมี ..... ลายมือชื่อนิสิต .....

สาขาวิชา ..... วิศวกรรมเคมี ..... ลายมือชื่อ อ. ที่ปรึกษาวิทยานิพนธ์หลัก .....

ปีการศึกษา ..... 2555 ..... ลายมือชื่อ อ. ที่ปรึกษาวิทยานิพนธ์ร่วม .....

# # 5470512221: MAJOR CHEMICAL ENGINEERING

KEYWORDS: HYDROPROCESSING / FATTY ACID / NiMo /NiMoW / CoMo / CoMOW / CARBIDATION

PONGSATORN JANTHARAK : EFFECT OF TUNGSTEN LOADING ON NiMo/Al<sub>2</sub>O<sub>3</sub> AND CoMo/Al<sub>2</sub>O<sub>3</sub> CATALYSTS FOR HYDROPROCESSING OF BIODIESEL PRODUCTION. ADVISOR: PROF. SUTTICHA ASSABUMRUNGRAT, Ph.D., CO-ADVISOR: ASST.PROF. WORAPON KIATKITTIPONG, D.Eng., 71 pp.

In this research, the effect of the addition of tungsten over NiMo and CoMo catalysts supported on alumina for biodiesel production via hydroprocessing was investigated. The experiment was operated at a temperature range of 300-400 °C, hydrogen pressure of 40 bar and reaction time from one to four hours using carbided NiMo and CoMo catalysts supported on alumina with and without addition of tungsten. Three types of fatty acid, including of oleic acid, stearic acid and palmitic acid were used as raw materials. From the experimental studies, it was found that addition of tungsten could promote activity and diesel selectivity for both NiMo and CoMo catalysts. Oligomerization products are observed at lower than 350°C with a short reaction time (normally less than 2 hours) while cracking products are mostly observed at high temperature and/or longer reaction time. The highest diesel yield of 66.9% was achieved for the hydroprocessing of oleic acid using NiMo with the addition of tungsten at 350°C, 40 bar and 2 hours. Liquid products contained hydrocarbons in a range of C<sub>15</sub>-C<sub>18</sub> and water while gaseous products were carbon monoxide, carbon dioxide and methane.

Department : .....Chemical Engineering.....Student's Signature .....

Field of Study : .....Chemical Engineering.....Advisor's Signature .....

Academic Year : .....2012.....Co-advisor's Signature .....

## ACKNOWLEDGEMENTS

The author would like to express his highest gratitude to Professor Suttichai Assabumrungrat, advisor and Assistant Professor Worapon Kiatkittipong, co-advisor for their inspiration, assistance and many good advices throughout the research study. Moreover, the author wishes to thank Assistant Professor Anongnat Somwangthanaroj, as the chairman, Assistant Professor Suphot Phatanasri, Associate Professor Navadol Laosiripojana as the members of the thesis committee.

Most of all, the author would like to express his highest gratitude to his parents who always pay attention to him all the times for their suggestion and have provided supports and encouragements. The most success of graduation is devoted to his parents.

Moreover, grateful thanks to members in Center of Excellence on Catalysis and Catalytic Reaction Engineering, Department of Chemical Engineering, Chulalongkorn University as well as Professor Piyasan Prasertdam. Special thanks to Mr.Watcharapong Khaowdee, Ms.Cholada Laokittikul, Ms.Boonwara Ngamlertkul, Ms.Wanna Phiwkliang, Ms. Boontida Pongthawornsakun and others not specifically named, who have provided his support and encouragement, please be assured that he thinks of you

Finally, the author would like to thank the Thailand Research Fund (TRF), as well as the Graduate School of Chulalongkorn University for their financial supports.

# CONTENTS

	PAGE
ABSTRACT IN THAI .....	iv
ABSTRACT IN ENGLISH.....	v
ACKNOWLEDGEMENTS .....	vi
CONTENTS.....	vii
LIST OF TABLES .....	x
LIST OF FIGURES .....	xi
CHAPTER I INTRODUCTION.....	1
1.1 Rationale.....	1
1.2 Objective .....	2
1.3 Scope of Work.....	3
1.4 Research Methodology.....	4
CHAPTER II THEORY .....	5
2.1 Mechanism of Hydroprocessing.....	5
2.1.1 Hydrogenation.....	5
2.1.2 Hydrodeoxygenation.....	7
2.1.3 Decarboxylation.....	7
2.1.4 Decarbonylation.....	7
2.1.5 Isomerization and Cracking .....	8
2.1.6 Water Gas Shift and Methanization.....	8
2.2 Metal and Support .....	8
2.2.1 Nickel.....	8
2.2.2 Cobolt.....	10
2.2.3 Molybdenum.....	11

2.2.4 Tungsten.....	12
2.2.5 Aluminium Oxides or Alumina ( $Al_2O_3$ ) .....	12
2.3 Metal Carbides and Nitrides Catalysts .....	13
CHAPTER III LITERATURE REVIEWS .....	15
3.1 Reaction Condition.....	15
3.2 Effect of the Operating Condition .....	15
3.3 Thermodynamic Balance.....	20
3.4 Catalyst.....	21
3.5 Properties of Production .....	22
CHAPTER IV EXPERIMENTAL .....	23
4.1 Chemicals .....	23
4.2 Catalysts Preparation.....	24
4.2.1 Preparation of NiMo-NiMoW/ $Al_2O_3$ and CoMo-CoMoW/ $Al_2O_3$ .....	24
4.3 Catalyst Characterization .....	25
4.3.1 X-ray Diffraction (XRD) .....	25
4.3.2 Nitrogen Physisorption (BET) .....	26
4.3.3 $H_2$ Temperature Programmed Reduction ( $H_2$ -TPR) .....	27
4.3.4 Inductively Coupled Plasma-Optical Emission Spectroscopy (ICP-OES).....	27
4.3.5 Ammonia Temperature Program Desorption ( $NH_3$ -TPD).....	28
CHAPTER V RESULTS AND DISCUSSION .....	29
5.1 Catalyst Characterization .....	29
5.1.1 Inductively Coupled Plasma-Optical Emission Spectroscopy (ICP-OES).....	29
5.1.2 $N_2$ Physisorption .....	30
5.1.3 X-ray Diffraction .....	31



5.1.4 H <sub>2</sub> Temperature-Programmed Reduction (H <sub>2</sub> -TPR).....	32
5.1.5 Ammonia Temperature Programmed Desorption (NH <sub>3</sub> -TPD).....	34
5.2 Hydrotreated Hydrogenation of Fatty Acid.....	36
5.2.1 Effect of Temperature and Reaction time on Conversion and Diesel Yield.....	38
5.2.2 Effect of Catalysts to Ratio of C <sub>n-1</sub> /C <sub>n</sub> Product.....	47
CHAPTER VI CONCLUSIONS AND RECOMMENDATIONS.....	49
6.1 Conclusions .....	49
6.2 Recommendations.....	50
REFERENCES.....	51
APPENDICES .....	53
APPENDIX A CALCULATION OF CATALYST PREPARATION .....	54
APPENDIX B CALIBRATION CURVE.....	59
APPENDIX C CALCULATION OF ACID SITE.....	64
APPENDIX D PRODUCTS DISTRIBUTION .....	66
APPENDIX E LIST OF PUBLICATION .....	70
VITA .....	71

**LIST OF TABLES**

TABLE	PAGE
5.1 ICP-OES analysis of element .....	29
5.2 Surface area, pore volume, and pore size of catalyst by N <sub>2</sub> physisorption .....	29
5.3 Ratio C17/C18 of Oleic acid .....	46
5.4 Ratio C17/C18 of Stearic acid.....	47
5.5 Ratio C15/C16 of Palmitic acid.....	47
B.1 Result from chromatogram of calibration mixture reference .....	61
B.2 Operating condition for gas chromatography.....	62
C.1 Data for calculation of total acid site.....	64

## LIST OF FIGURES

FIGURE	PAGE
2.1 Mechanism pathway of hydrogenation .....	5
2.2 Activation energy of hydrogenation.....	5
2.3 Mechanism pathway of hydrodeoxygenation.....	6
2.4 Thermal transformation of difference type of starting material .....	12
2.5 Crystallographic structure of Mo <sub>2</sub> C, Mo <sub>2</sub> N and MoS <sub>2</sub> .....	13
4.1 Show the flow diagram of synthesis metal carbide and presulfided catalyst.....	23
5.1 XRD pattern of NiMo/Al <sub>2</sub> O <sub>3</sub> and NiMoW/ Al <sub>2</sub> O <sub>3</sub> .....	30
5.2 XRD pattern of CoMo/Al <sub>2</sub> O <sub>3</sub> and CoMoW/ Al <sub>2</sub> O <sub>3</sub> .....	31
5.3 H <sub>2</sub> -TPR of NiMo/Al <sub>2</sub> O <sub>3</sub> and NiMoW/ Al <sub>2</sub> O <sub>3</sub> .....	32
5.4 H <sub>2</sub> -TPR of CoMo/Al <sub>2</sub> O <sub>3</sub> and CoMoW/ Al <sub>2</sub> O <sub>3</sub> .....	33
5.5 NH <sub>3</sub> TPD of NiMo/Al <sub>2</sub> O <sub>3</sub> and NiMoW/ Al <sub>2</sub> O <sub>3</sub> .....	34
5.6 NH <sub>3</sub> TPD of CoMo/Al <sub>2</sub> O <sub>3</sub> and CoMoW/ Al <sub>2</sub> O <sub>3</sub> .....	34
5.7 Conversion and diesel yield of oleic acid on CoMo/ $\gamma$ Al <sub>2</sub> O <sub>3</sub> catalyst with H <sub>2</sub> pressure 40 bar .....	38
5.8 Conversion and diesel yield of oleic acid on CoMoW/ $\gamma$ Al <sub>2</sub> O <sub>3</sub> catalyst with H <sub>2</sub> pressure 40 bar .....	38
5.9 Conversion and diesel yield of oleic acid on NiMo/ $\gamma$ Al <sub>2</sub> O <sub>3</sub> catalyst with H <sub>2</sub> pressure 40 bar .....	39
5.10 Conversion and diesel yield of oleic acid on NiMoW/ $\gamma$ Al <sub>2</sub> O <sub>3</sub> catalyst with H <sub>2</sub> pressure 40 bar .....	39

5.11 Conversion and diesel yield of stearic acid on CoMo/ $\gamma$ Al <sub>2</sub> O <sub>3</sub> catalyst with H <sub>2</sub> pressure 40 bar .....	40
5.12 Conversion and diesel yield of stearic acid on CoMoW/ $\gamma$ Al <sub>2</sub> O <sub>3</sub> catalyst with H <sub>2</sub> pressure 40 bar .....	41
5.13 Conversion and diesel yield of stearic acid on NiMo/ $\gamma$ Al <sub>2</sub> O <sub>3</sub> catalyst with H <sub>2</sub> pressure 40 bar.....	41
5.14 Conversion and diesel yield of stearic acid on NiMoW/ $\gamma$ Al <sub>2</sub> O <sub>3</sub> catalyst with H <sub>2</sub> pressure 40 bar.....	42
5.15 Conversion and diesel yield of palmitic acid on CoMo/ $\gamma$ Al <sub>2</sub> O <sub>3</sub> catalyst with H <sub>2</sub> pressure 40 bar.....	43
5.16 Conversion and diesel yield of palmitic acid on CoMoW/ $\gamma$ Al <sub>2</sub> O <sub>3</sub> catalyst with H <sub>2</sub> pressure 40 bar.....	44
5.17 Conversion and diesel yield of palmitic acid on NiMo/ $\gamma$ Al <sub>2</sub> O <sub>3</sub> catalyst with H <sub>2</sub> pressure 40 bar.....	44
5.18 Conversion and diesel yield of palmitic acid on NiMoW/ $\gamma$ Al <sub>2</sub> O <sub>3</sub> catalyst with H <sub>2</sub> pressure 40 bar.....	45
B.1 Calibration curve of Oleic acid .....	59
B.2 Calibration curve of Stearic acid .....	60
B.3 Calibration curve of Palmitic acid.....	60
B.4 Chromatogram of calibration mixture reference .....	61
C.1 The calibration curve of ammonia.....	65
D.1 Product distribution of stearic acid obtain from CoMo/ $\gamma$ Al <sub>2</sub> O <sub>3</sub> catalyst under H <sub>2</sub> pressure of 40 bar .....	66

D.2 Product distribution of stearic acid obtain from CoMoW/ $\gamma$ Al <sub>2</sub> O <sub>3</sub> catalyst under H <sub>2</sub> pressure of 40 bar .....	66
D.3 Product distribution of stearic acid obtain from NiMo/ $\gamma$ Al <sub>2</sub> O <sub>3</sub> catalyst under H <sub>2</sub> pressure of 40 bar .....	67
D.4 Product distribution of stearic acid obtain from NiMoW/ $\gamma$ Al <sub>2</sub> O <sub>3</sub> catalyst under H <sub>2</sub> pressure of 40 bar .....	67
D.5 Product distribution of palmitic acid obtain from CoMo/ $\gamma$ Al <sub>2</sub> O <sub>3</sub> catalyst under H <sub>2</sub> pressure of 40 bar .....	68
D.6 Product distribution of palmitic acid obtain from CoMoW/ $\gamma$ Al <sub>2</sub> O <sub>3</sub> catalyst under H <sub>2</sub> pressure of 40 bar .....	68
D.7 Product distribution of palmitic acid obtain from NiMo/ $\gamma$ Al <sub>2</sub> O <sub>3</sub> catalyst under H <sub>2</sub> pressure of 40 bar .....	69
D.8 Product distribution of palmitic acid obtain from NiMoW/ $\gamma$ Al <sub>2</sub> O <sub>3</sub> catalyst under H <sub>2</sub> pressure of 40 bar .....	69

# CHAPTER I

## INTRODUCTION

### 1.1 Rationale

Biodiesel is an important alternative fuel made from renewable resources such as vegetable oils or animal fat. The main reason of the consumption of biofuels within the alternative fuels is the insufficient quantity and availability of energy in a part of transportation to reduce the dependence on petroleum from import crude oil and to decrease the environmental problem (Krár et al 2010). FAMEs (fatty acid methyl ester) is biodiesel from trans-esterification process of vegetable oil that is called “First generation biodiesel”. There are still many drawbacks of biodiesel based on FAMEs, such as lower heating value of the blends and compatibility problems with some components in vehicles (Sankaranarayanan et al 2011). The next generation of biodiesel is produced from hydroprocessing processes of vegetable oil which is call “Second generation biodiesel”. The catalytic hydroprocessing is an alternative conversion technology of liquid biomass to biofuels which is lately raising a number of interestes in both the academic and industrial sections. The hydrodeoxygenation is suitable for converting low-grade waste oils into hydrocarbons which are similar to the components in the petroleum diesel (Toba et al 2011). The hydrodeoxygenation reactions of fatty acids accompanied with catalysts could produce biofuels products with increasing cetane number, heating value and oxidation stability (Bezergianni et al 2012).

The catalysts for producing the biodiesel from hydroprocessing process have been developed in recent year in order to increase the efficiency of process and the quality of biodiesel. The studies of metal and the catalyst support to use with varions raw material for producing the biodiesel have been considered.

The conventional catalysts for hydroprocessing of vegetable oil are NiMo/Al<sub>2</sub>O<sub>3</sub> and CoMo/Al<sub>2</sub>O<sub>3</sub>. A bimetallic catalyst is typically used which has a metal acting as a catalyst promoter, often cobalt or nickel, and another metal, often tungsten or molybdenum, providing the active sites necessary for the catalytic conversion. Sulfide is generally employed as the active phase for the metal catalyst by forming MoS<sub>2</sub>/WS<sub>2</sub> crystal structures.

More recently, the potential of applying trimetallic NiMoW catalysts for hydrotreating has been explored. Nava et al and Absi-Halabi et al have reported NiMoW/Al<sub>2</sub>O<sub>3</sub> sulfide catalysts having higher HDS activity when compared with NiMo/Al<sub>2</sub>O<sub>3</sub> and NiW/Al<sub>2</sub>O<sub>3</sub> sulfide catalysts (Absi-Halabi et al) led to the patenting of an unsupported NiMoW catalyst named NEBULA, which was found to have far greater HDS activity than supported bimetallic catalysts (Sigurdson et al 2008).

In this study, The fatty acids was performed in a shaking batch reactor under condition of temperature of 300 – 400 °C, hydrogen pressure of 40 bar and reaction time 1-4 h catalyzed by NiMo/Al<sub>2</sub>O<sub>3</sub>, NiMoW/Al<sub>2</sub>O<sub>3</sub>, CoMo/Al<sub>2</sub>O<sub>3</sub> CoMoW/Al<sub>2</sub>O<sub>3</sub> carbides in-house prepared catalysts. Liquid reaction products are hydrocarbons whose main components were identified as C<sub>15</sub> - C<sub>18</sub> alkanes. The yield of diesel (range 300 – 400 °C). It can be concluded that the products are suitable for diesel fuel blending. Influence of operating condition and catalyst on the product compositions in the case of fatty acid as starting materials is also discussed (Filho et al., 1993).

## **1.2 Objective**

Find the suitable condition for catalyst that doping of tungsten to use in hydroprocessing process.

### 1.3 Scope of Work

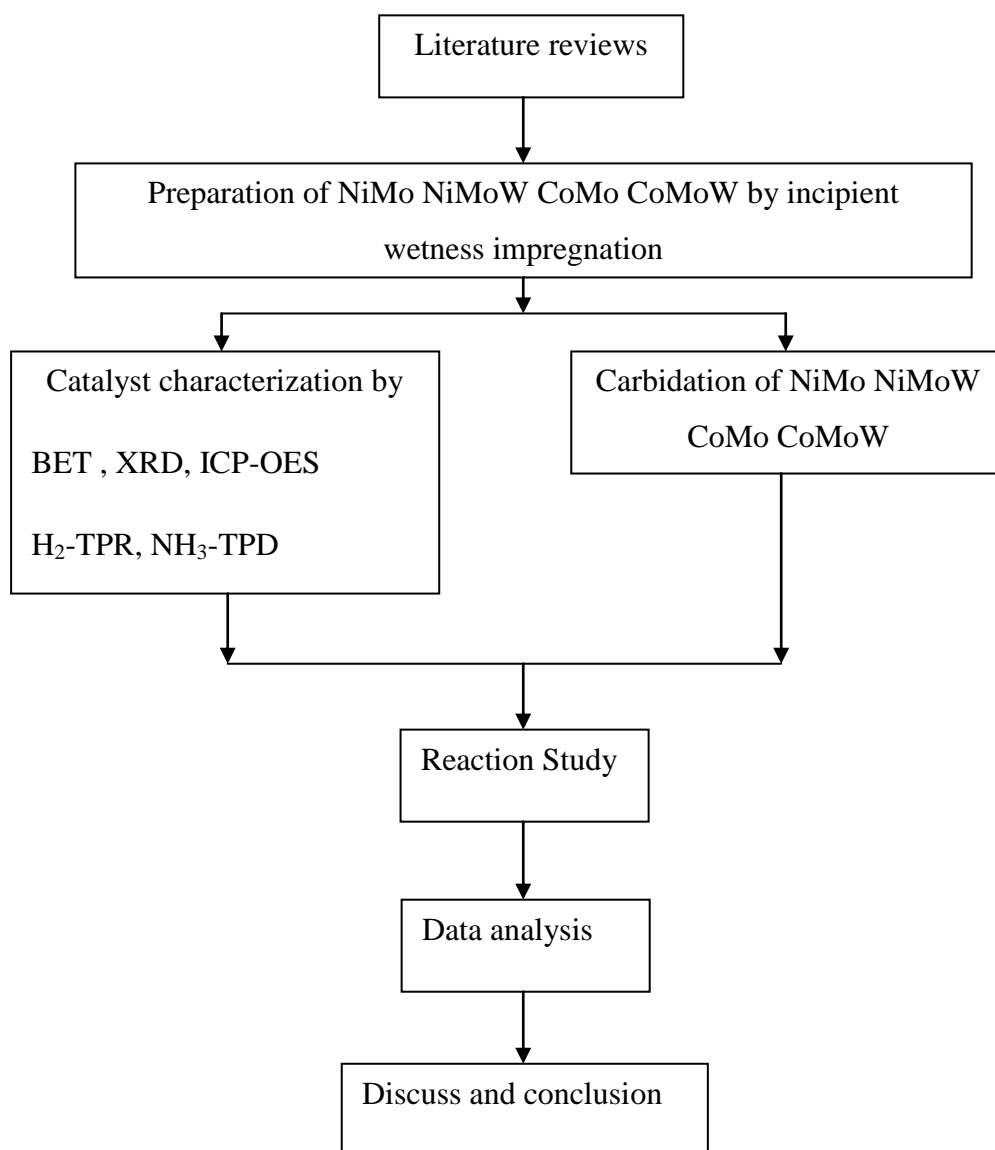
1. Prepare the trimetallic NiMoW/Al<sub>2</sub>O<sub>3</sub> CoMoW/Al<sub>2</sub>O<sub>3</sub> and bimetallic NiMo/Al<sub>2</sub>O<sub>3</sub> CoMo/Al<sub>2</sub>O<sub>3</sub> carbide catalyst.

2. Characterization of catalyst include of Brunauer-Emmett-Teller (BET) for surface area analysis Inductively coupled Plasma-Optical Emission Spectroscopy (ICP-OES), X-ray diffraction (XRD), temperature-programmed reduction of hydrogen (H<sub>2</sub>-TPR) and ammonia temperature program desorption (NH<sub>3</sub>-TPD).

3. The liquid product from reaction was analyzed by Shimadzu GC-14B gas chromatograph equipped with an Agilent DB-2887 column to examine product distribution. Gas product was analyzed by using gas chromatography with thermal conductivity detector (TCD).



## 1.4 Research Methodology



## CHAPTER II

### THEORY

In this chapter will expand about research review which is relate to produce biodiesel with hydroprocessing process, fatty acid mechanism, property of diesel production and metal carbides catalyst

#### 2.1 Mechanism of Hydroprocessing

Hydroprocessing process study about reaction of hydrodenitrogenation(HDN), hydrodesulfurization(HDS), hydrodeoxygenation(HDO), hydrogenation(HDY) and hydrodemetallization(HDM)

##### 2.1.1 Hydrogenation (<http://chemwiki.ucdavis.edu/>)

The processes that treat with hydrogen call hydrogenation. It's show the chemical reaction between hydrogen ( $H_2$ ) molecule and another compound or element that usually in the presence of a catalyst. The process is commonly reduces or saturate organic compounds. Hydrogenation typically constitutes the addition of pairs of hydrogen atoms to a molecule in general is an alkenes. Catalysts are required for the reaction to catalyze reaction. The non-catalytic hydrogenation takes place only at very high temperatures. Hydrogen adds to double and triple bonds in hydrocarbons. The reverse reaction, removal of hydrogen from a molecule is called dehydrogenation. A reaction where bonds are broken while hydrogen is add call hydrogenolysis. The reaction may occur with carbon-carbon atoms and carbon-heteroatom (oxygen, nitrogen or halogen) bonds. Hydrogenation differs from protonation or hydride addition: in hydrogenation, the products have the same charge as the reactants. This process is show how the catalyst remove double bond from molecule with hydrogen in figure 2.1

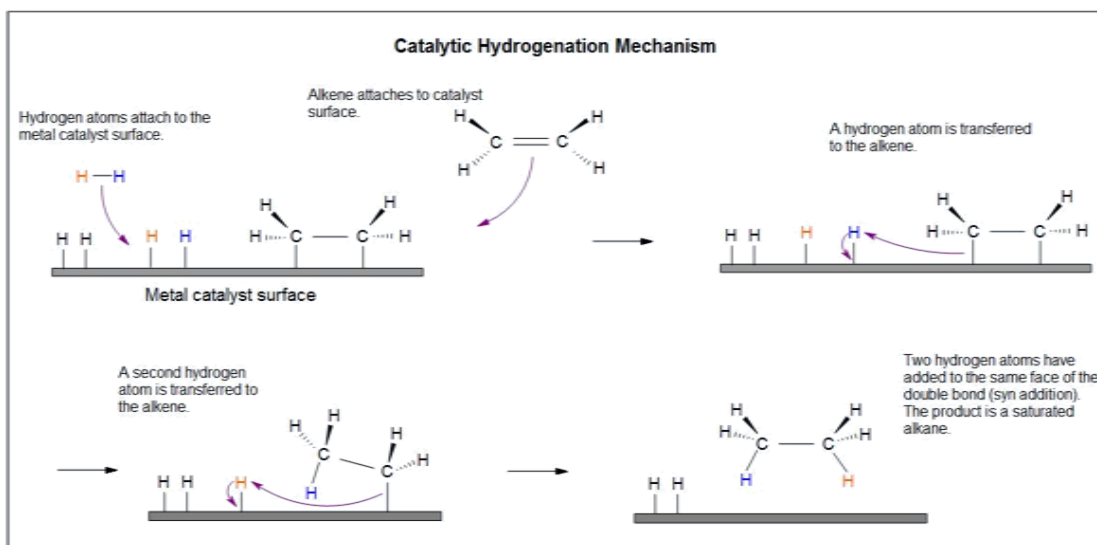
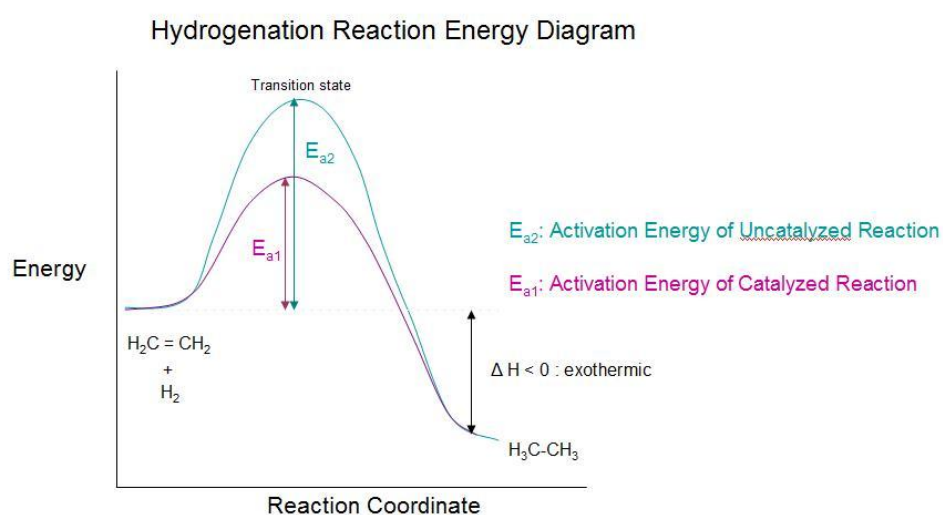


**Figure 2.1** Mechanism pathway of hydrogenation

Hydrogenation of a double bond is a thermodynamically favorable reaction because it forms a more stable (lower energy) product. In other words, the energy of the product is lower than the energy of the reactant; thus it is exothermic (heat is released). The heat released is called the heat of hydrogenation, which is an indicator of a molecule's stability.



A catalyst lowers the activation energy needed for the reacting molecules to reach the transition state. The addition of a catalyst enables the hydrogenation reaction to occur, that otherwise, would not.

**Figure 2.2** Activation energy of hydrogenation

### 2.1.2 Hydrodeoxygenation (<http://en.wikipedia.org/wiki>)

Hydrodeoxygenation (HDO) is a hydrogenolysis process for removing oxygen from compounds. It is of interest for biofuels which are derived from oxygen-rich precursors like fatty acids. Typical HDO catalysts commonly are nickel-molybdenum or cobalt-molybdenum on gamma alumina. The summarized reactions are showed as follows in figure 2.3

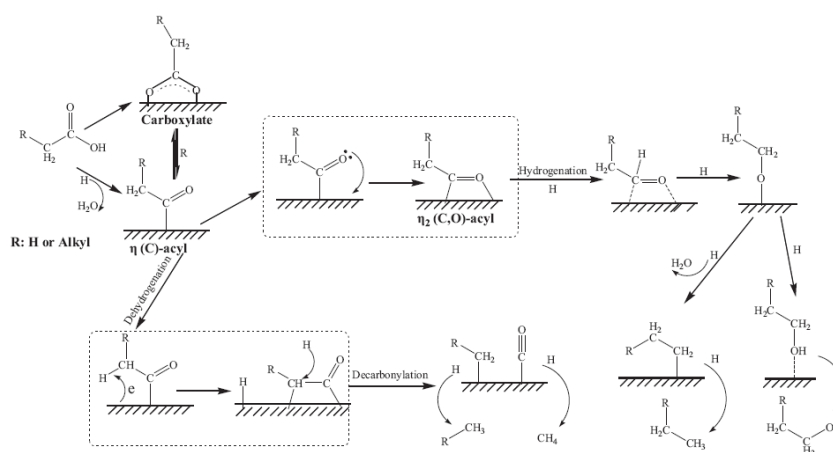


**Figure 2.3** Mechanism pathway of hydrodeoxygenation

### 2.1.3 Decarboxylation (<http://en.wikipedia.org/wiki>)

Decarboxylation is a chemical reaction that releases carbon dioxide ( $CO_2$ ) from a carboxylic group, almost any carboxylic acid. A reaction of carboxylic acids removing a carbon atom from a carbon chain when heat to a very high temperature, undergoes thermal decarboxylation. The removing a carbon atom from a carbon chain without hydrogen required to convert a carboxylic acid group to an alkane.

### 2.1.4 Decarbonylation

The decarbonylation is chemical reaction which the carboxylic group is reacted with hydrogen for removal one or more carbonyl groups from a molecule to produce a methyl group, carbon monoxide and water (Donnis et al 2009; Mikulec et al 2010)

### 2.1.5 Isomerization and Cracking

The normal alkanes produced from triglyceride can undergo isomerization and cracking to produce isomerized and lighter alkanes, respectively. The normal alkanes have a high cetane number, which is a good for diesel production. If the normal alkanes are desired then the isomerization and cracking reactions should be minimized (Huber et al 2007).

### 2.1.6 Water Gas Shift and Methanization

The water-gas shift reaction (WGS) is a chemical reaction in which carbon monoxide reacts with water vapor to form carbon dioxide and hydrogen



The water-gas shift reaction was discovered by Italian physicist Felice Fontana in 1780. The reaction is slightly exothermic, yielding 41.1 kJ (10 kcal) per mole

Methanation is a physical-chemical process to generate Methane from a mixture of various gases by thermo-chemical gasification. The main components are carbon monoxide and hydrogen or carbon dioxide and hydrogen. The main catalysts used for this reaction are ruthenium, cobalt, nickel and iron. The following main process describes the methanation



## 2.2 Metal and Support

### 2.2.1 Nickel (<http://en.wikipedia.org/wiki/>)

Nickel is a chemical element with the chemical symbol Ni and atomic number 28. It is a silvery-white lustrous metal with a slight golden tinge. Nickel belongs to the transition metals and is hard and ductile. Pure nickel shows a significant chemical activity that can be observed when nickel is powdered to maximize the exposed surface area on which reactions can occur but larger pieces of the metal are slow to

react with air at ambient conditions due to the formation of a protective oxide surface. Nickel is reactive enough with oxygen so that native nickel is rarely found on Earth's surface being mostly confined to the interiors of larger nickel–iron meteorites that were protected from oxidation during their time in space. Native nickel is always found in combination with iron, a reflection of those elements' origin as major end products of supernova nucleosynthesis. An iron–nickel mixture is thought to compose Earth's inner core.

The use of nickel (as a natural meteoric nickel–iron alloy) has been traced as far back as 3500 BC. Nickel was first isolated and classified as a chemical element in 1751 by Axel Fredrik Cronstedt, who initially mistook its ore for a copper mineral. The element name comes from a mischievous sprite of German miner's mythology, Nickel (similar to Old Nick), that personified the fact that copper-nickel ores resisted refinement into copper. Nickel's most important modern ore minerals are laterites, including limonite, garnierite, and pentlandite. Major production sites include Sudbury region in Canada (which is thought to be of meteoric origin), New Caledonia in the Pacific and Norilsk in Russia.

Because of nickel's slow rate of oxidation at room temperature, it is considered corrosion-resistant. Historically this has led to its use for plating metals such as iron and brass, to its use for chemical apparatus, and its use in certain alloys that retain a high silvery polish, such as German silver. About 6% of world nickel production is still used for corrosion-resistant pure-nickel plating. Nickel was once a common component of coins, but has largely been replaced by cheaper iron for this purpose, especially since the metal is a skin allergen for some people.

Nickel is one of four elements that are ferromagnetic around room temperature. Alnico permanent magnets based partly on nickel are of intermediate strength between iron-based permanent magnets and rare-earth magnets. The metal is chiefly valuable in the modern world for the alloys it forms; about 60% of world production is used in nickel-steels (particularly stainless steel). Other common alloys, as well as some new superalloys, make up most of the remainder of world nickel use, with chemical uses for nickel compounds consuming less than 3% of production. As a

compound, nickel has a number of niche chemical manufacturing uses, such as a catalyst for hydrogenation. Enzymes of some microorganisms and plants contain nickel as an active site, which makes the metal an essential nutrient for them.

### **2.2.2 Cobalt** (<http://en.wikipedia.org/wiki/>)

Cobalt is a chemical element with symbol Co and atomic number 27. It is found naturally only in chemically combined form. The free element, produced by reductive smelting, is a hard, lustrous, silver-gray metal.

Cobalt-based blue pigments (cobalt blue) have been used since ancient times for jewelry and paints, and to impart a distinctive blue tint to glass, but the color was later thought by alchemists to be due to the known metal bismuth. Miners had long used the name kobold ore (German for goblin ore) for some of the blue-pigment producing minerals; they were named because they were poor in known metals and gave poisonous arsenic-containing fumes upon smelting. In 1735, such ores were found to be reducible to a new metal (the first discovered since ancient times), and this was ultimately named for the kobold.

Today, some cobalt is produced specifically from various metallic-lustered ores, for example cobaltite (CoAsS), but the main source of the element is as a by-product of copper and nickel mining. The copper belt in the Democratic Republic of the Congo and Zambia yields most of the cobalt metal mined worldwide.

Cobalt is used in the preparation of magnetic, wear-resistant and high-strength alloys. Cobalt silicate and cobalt(II) aluminate ( $\text{CoAl}_2\text{O}_4$ , cobalt blue) give a distinctive deep blue color to glass, smalt, ceramics, inks, paints and varnishes. Cobalt occurs naturally as only one stable isotope, cobalt-59. Cobalt-60 is a commercially important radioisotope, used as a radioactive tracer and in the production of gamma rays.

Cobalt is the active center of coenzymes called cobalamins, the most common example of which is vitamin B<sub>12</sub>. As such it is an essential tracedietary mineral for all

animals. Cobalt in inorganic form is also an active nutrient for bacteria, algae and fungi.

### 2.2.3 Molybdenum (<http://en.wikipedia.org/wiki/>)

Molybdenum is a Group 6 chemical element with the symbol Mo and atomic number 42. The name is from Neo-Latin Molybdaenum, from Ancient Greek Μόλυβδος molybdos, meaning lead, since its ores were confused with lead ores. Molybdenum minerals have been known into prehistory, but the element was "discovered" (in the sense of differentiating it as a new entity from the mineral salts of other metals) in 1778 by Carl Wilhelm Scheele. The metal was first isolated in 1781 by Peter Jacob Hjelm.

Molybdenum does not occur naturally as a free metal on Earth, but rather in various oxidation states in minerals. The free element, which is a silvery metal with a gray cast, has the sixth-highest melting point of any element. It readily forms hard, stable carbides in alloys, and for this reason most of world production of the element (about 80%) is in making many types of steel alloys, including high strength alloys and superalloys.

Most molybdenum compounds have low solubility in water, but the molybdate ion  $\text{MoO}_4^{2-}$  is soluble and forms when molybdenum-containing minerals are in contact with oxygen and water. Industrially, molybdenum compounds (about 14% of world production of the element) are used in high-pressure and high-temperature applications, as pigments and catalysts.

Molybdenum-containing enzymes are by far the most common catalysts used by some bacteria to break the chemical bond in atmospheric molecular nitrogen, allowing biological nitrogen fixation. At least 50 molybdenum-containing enzymes are now known in bacteria and animals, although only bacterial and cyanobacterial enzymes are involved in nitrogen fixation, and these nitrogenases contain molybdenum in a different form from the rest. Owing to the diverse functions of the various other types of molybdenum enzymes, molybdenum is a required element for life in all higher organisms (eukaryotes), though not in all bacteria.



#### 2.2.4 Tungsten (<http://en.wikipedia.org/wiki/>)

Tungsten, also known as wolfram, is a chemical element with the chemical symbol W and atomic number 74. The word tungsten comes from the Swedish language tung sten directly translatable to heavy stone, though the name is volfram in Swedish to distinguish it from Scheelite, in Swedish alternatively named tungsten.

#### 2.2.5 Aluminium Oxides or Alumina ( $\text{Al}_2\text{O}_3$ )

It is well known that alumina is a term of alumina compounds. Also, alumina has a number of crystalline phases, in generally, alumina can exist in many metastable phase before transforming to the stable form of alumina in which the stable form of alumina was well known as  $\alpha$ -alumina form or corundum form. There are six principle phase designated by the Greek letters, composed that chi ( $\chi$ ), kappa ( $\kappa$ ), eta ( $\eta$ ), theta ( $\theta$ ), delta ( $\delta$ ), and gamma ( $\gamma$ ). The nature of the product obtained depending on many factors such as calcination temperature, heating environment, as one can so-called heat treatment conditions. In addition, starting hydroxide such as gibbsite, boehmite and others could be affecting to the nature of the product, which can be illustrated in Figure 2.4, which shows thermal transformation scheme of different types of starting material. As can be seen, among the various crystalline phases of alumina,  $\gamma$ - $\text{Al}_2\text{O}_3$  is probably the most important inorganic oxide refractory of widespread technological importance in the field of catalysis, also used as catalyst support. In addition,  $\gamma$ - $\text{Al}_2\text{O}_3$  is an exceptionally good choice for catalytic applications because of a defect spinel crystal lattice that imparts to it a structure that is both open and capable of high surface area (Yang 2007).

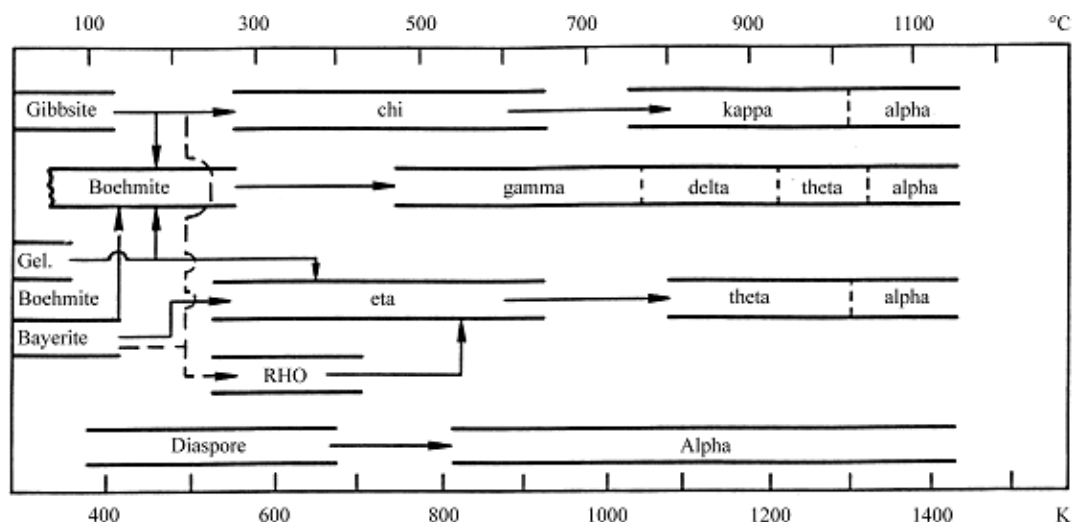


**Figure 2.4** Thermal transformations of different types of starting material (Santos et al 2000)

### 2.3 Metal Carbides and Nitrides Catalysts

Sulfides from of molybdenum with cobalt and nickel promoter have traditionally been catalysts for hydrotreating reactions. Currently, petroleum refining industry has been facing significant challenging due to the decreasing allowable amount of emissions, such as  $\text{SO}_x$ ,  $\text{NO}_x$  and aromatics from the combustion of fuels. This may include a substantial increase in the amount of conventional catalysts, decreasing daily throughputs, increasing the consumption of  $\text{H}_2$ , etc. Since the last decade, there have many efforts to develop such catalysts for hydroprocessing. Metal carbides and nitrides have been identified as the potential catalysts for such applications. Regarding to Mo based solid have been receiving most of the attention such that Mo nitrides, the volume of information is much more extensive than that on Mo carbides (Furimsky 2003).

The properties and the information on structure for Mo carbides and nitrides is shown in Figure 2.5 which illustrates fundamental difference between the structures of Mo carbides and nitrides compared with that of  $\text{MoS}_2$  (Sajkowski & Oyama 1996).

The elementary theory of these compounds suggests that the introduction of carbon or nitrogen into the lattice of the early transition metals results in an increase of the lattice parameter  $a_0$ . Molybdenum carbides and nitrides are characterized by the hexagonal close-packed and body-centered cubic crystal structure, respectively

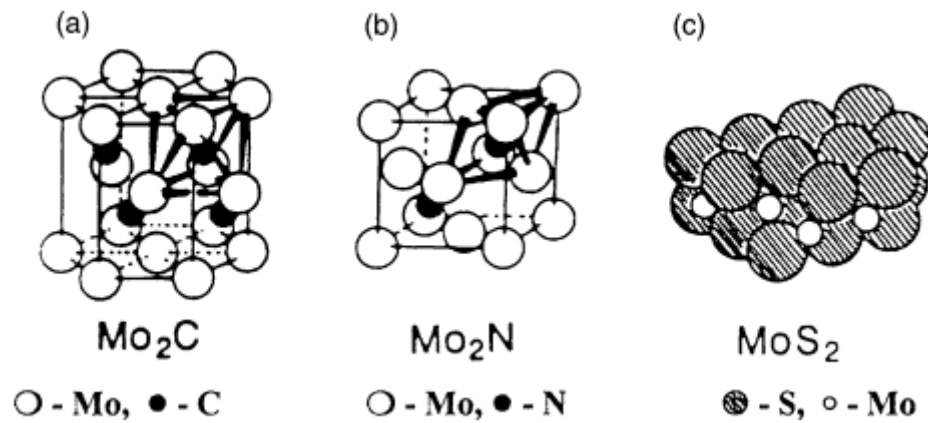


**Figure 2.5** Crystallographic structure of  $\text{Mo}_2\text{C}$ ,  $\text{Mo}_2\text{N}$  and  $\text{MoS}_2$  (Sajkowski, and Oyama., 1996).

## **CHAPTER III**

### **LITERATURE REVIEWS**

This chapter showed the review of research that related to produce of the second generation of biodiesel. Which the suitable operating condition and catalysts

#### **3.1 Reaction Condition**

This study describes the three carboxylic acids are stepwise liberated and hydrogenated into straight chain alkanes of the same length or one carbon atom shorter. Byproducts are water, carbon monoxide, carbon dioxide and methane. These products will be considerable due to appropriated conditions and suitable catalyst. The proposed reaction mechanism, which can be explained the path way of these products, involve at least three reaction pathways as hydrodeoxygenation, decarboxylation and decarbonylation.

#### **3.2 Effect of the Operating Condition**

Temperatures, hydrogen pressure, time of stream and catalysts have been identified as a key parameter for catalyst effectiveness and catalyst life. Increasing temperature increases catalyst activity and increasing catalyst activity causes a faster decay of catalyst life.

The effect of temperature was studied at 350, 370 and 390°C, the conversion and product yields are estimated from the simulated distillation data of the total liquid product at the each temperature. The produced liquid biofuels (gasoline and diesel) increase. This is expected as hydrocracking activity rises with increasing temperature. Furthermore gasoline yield increases monotonically with temperature, while diesel yield is smaller at the middle temperature (370°C) (Bezergianni & Kalogianni 2009). The minimum diesel yield observed at 370°C is attributed to the fact that increasing

temperature. The cracking reactions favored by increasing temperature. These hydrocracking reactions convert heavier molecules including some diesel molecules into lighter gasoline molecules. After that (Bezergianni et al 2010) was observed that as the temperature increases the amount of paraffins decrease, while the amount of iso-paraffins increases. The decrease of n-paraffins vs. the increase of iso-paraffins indicate that isomerization reactions are favored by hydrotreating temperature, which is expected as higher temperatures because hydrocracking type of reactions (which include isomerization and cracking).

The study of SHP technology by Tailleux in 2006 which is develops of diesel hydrotreating unit in a conventional diesel hydroreactor (HDT). It was found that low sulfur low aromatics diesel and enhancing selectivity toward to light parafin and naphthene formation can obtain for this process. Moreover, the lower emission of pollution including  $\text{NO}_x$  and PM as well as the better in cetane number were observed. Finally, rate of reaction with respect to the lump of 11 gases and liquid phase reaction for hydroprocessing process was determined by the simplified kinetic model in order to optimize the investment cost of this catalytic system (Tailleux 2006). After that Sebos et al was tested the hydrodeoxygenation of mixture of 10 wt% cottonseed oil in diesel used in conventional hydrodesulphurization units of refinery plants. The product of renewable diesel has almost the same behavior as desulphurized diesel.(Sebos et al 2009)

The hydroprocessing was conducted by feed 0, 15 and 25 vol% rapeseed oil in light gas oil (LGO) with reaction temperature  $350^\circ\text{C}$  and under hydrogen pressure of 45 bar. A commercial TK-565 (Ni-Mo based) catalyst was used. The products obtain 100% conversion from rapeseed oil, the same final boiling point (FBP) of all three products were analyzed by the simulated distillation curves, which is also the FBP of the LGO feed. The HDO route and the decarboxylation route can be calculated from the yields of  $\text{CO}$ ,  $\text{CO}_2$ , and  $\text{CH}_4$ . The triglycerides reacted via the decarboxylation rate about 66-74%. Increased rapeseed oil mixed in LGO, properties of the diesel product were a low density and a high cetane index. The cloud point is important because the car manufactures observed filter plugging from the tank to the engine when operated at low temperatures. Therefore, the production of rapeseed oil will be improved

product properties as concern cloud and pour point (Donnis et al 2009). In the same year (Walendziewski et al 2009) studied hydroprocessing of 10 and 20 wt.% of rape oil and 90 and 80 wt.% of LGO fraction mixtures in continuous reactor with the same parameter sets, temperature 320, 350 and 380°C as well as under hydrogen pressure 3 and 5 MPa. A commercial NiMo/Al<sub>2</sub>O<sub>3</sub> catalyst was used. As the result of process the temperature range 350-380°C and hydrogen pressure 5 MPa are good efficiency. In comparison to the product yields for hydrotreating of vegetable oil (sunflower oil) used simulated distillation to analyze with the same as catalyst, temperature and pressure. It was obtained the maximum theoretical products carbon yields and carbon yields of C<sub>15</sub>-C<sub>18</sub> are 95% and 75%, respectively. The yields of gaseous (propane, carbon monoxide and carbon dioxide), isomerized and cracked products are minimum at the same temperature.(Huber et al 2007) The obtained liquid product was approximately 95 wt% yields of all products and 5 wt% of gaseous light hydrocarbons. Hydrogenation of unsaturated hydrocarbons and hydrogenolysis reactions of ester and carboxyl acid bonds results in fatty acid chains were converted to saturated linear hydrocarbon (paraffins), which are higher melting temperatures. It leads to undesirable increasing in boiling point, cloud point and CFPP. Bromine number decreased but acid number increased because ester bonds in fatty acids was hydrogenolized giving carboxylic group, which is loss because of hydrogenation of the carbonyl group (da Rocha Filho et al 1993). Then partial hydrocracking of paraffins hydrocarbons were transformed to light hydrocarbons whose flash point, density and kinematics viscosity are lower. There are improvement by the separation and removal of low boiling hydrocarbons from the product distillation.

The product yields for hydrotreating of vegetable oil used the simulated distillation to analyze. If at temperature less than 350°C was observed in products which contained small amounts of reaction intermediate and reactant. It was obtained that temperature at 350°C is suitable due to no oxygenated compounds and achieved 100% conversion (Šimáček et al 2010), the maximum theoretical products carbon yields and carbon yields of C<sub>15</sub>-C<sub>18</sub> are 95% and 75%, respectively. The yields of gaseous (propane, carbon monoxide and carbon dioxide), isomerized and cracked products are minimum (Huber et al 2007). It was observed by GC-MS when pressure

is decreased to 15 bar, product yields from n-C<sub>16</sub> to n-C<sub>18</sub> was increased due to increasing number of products and cannot specified exactly products like octadecenes, octadecanol, n-hexadecanoic acid, actadecanal and hexa-actadecyl hexadecanoate so there are several intermediates of this reactions. On the other hand, when pressure is increased (90 bar), decreasing number of products can be indentified because intermediates were not found and fatty acids is reduced as well. Subsequently, pressure effect and hydrogen consumption were tested via simulated in Aspen plus. It was found that the hydrodeoxygenation reaction is better than decarboxylation and decarbonylation when pressure increased and increasing hydrogen consumption. Moreover, time analysis was obtained by simulated distillation curves, the best diesel yields (95.3 % vol) was observed at 4 hours (Guzman et al 2010)

The product from the studied of hydroprocessing which rapeseed oil various at temperatures 260-340°C and under hydrogen pressure of 7 MPa. Three Ni-Mo/alumina hydrorefining catalysts were used. Reaction products contained water, hydrogen-rich gas and organic liquid product (OLP) (Šimáček et al 2009). At low reaction temperature (260-300°C), the OLP contained also reactant and intermediates (mainly triglycerides and free fatty acids). At reaction temperature higher than 310°C, the OLP contained mostly hydrocarbon (n-C<sub>17</sub> and n-C<sub>18</sub>). The reaction temperature is increased the content of n-C<sub>17</sub> increases and n-C<sub>18</sub> decreases. The OLP contained amount of i-alkanes (up to 40 wt.%) in the case of catalyst that consist of NiO 2.6 wt.% and MoO<sub>3</sub> 15.7 wt.%. It could improve low-temperature properties of the product. In 2010 he study again about hydroprocessing of rapeseed oil under reaction conditions at temperatures 310 and 360°C and under hydrogen pressure 7 and 15 MPa. A commercial hydrotreating Ni-Mo/alumina catalyst was used. The conversion of rapeseed oil was > 99% at 310°C because of observed in products contained small amounts of reaction intermedia (mainly stearic acid) and reactant. Trace on n-octadecanol, another reaction intermediate. At 360°C contained no oxygenated compounds, conversion was achieved 100%. Reaction products yields contained organic liquid product (OLP) -83 wt%, water-11 wt% and gaseous hydrocarbon- 6 wt%, the reaction gas contained propane, carbon dioxide, carbon monoxide and methane. The main of OLP are n-heptadecane and n-octadecane more than 75 wt% of all OLP. Beside other n-alkanes, iso-alkanes and cycloalkanes. Formation of i-alkanes

was increased when increasing reaction temperature and hydrogen pressure. Approximately 80% of all four products distilled at a boiling point of about 300-310°C were analyzed by the simulated distillation curves, which is falling into the diesel fuel distillation range. The kinematics viscosity was acceptable but the density was a little lower than diesel fuel. The cetane number can exceed the value of 100. Acid number increased at 310°C due to carboxylic group content. The parameters (Cloud point, pour point and CFPP) are main disadvantage of OLPs at low-temperature properties (Šimáček et al 2010). Which can prevent by utilization. (Šimáček & Kubička 2010) studied hydrocracking of pure petroleum vacuum distillate and the same fraction containing 5 wt% of rapeseed oil at temperatures 400 and 420°C and under hydrogen pressure of 18 MPa over commercial Ni-Mo. At 400°C the product of co-processing contained larger amount of n-C<sub>17</sub> and n-C<sub>18</sub> than the product from rapeseed-oil-free raw material. The high concentration of n-alkane resulted in worse low-temperature properties. On the other hand larger formation of i-alkane at 420°C decreased the content of n-C<sub>17</sub> and n-C<sub>18</sub>. The low-temperature properties of product were improved (Cloud point and CFPP).

The hydrodecarboxylation (HDC) reaction is favored by lower hydrogen pressure 35-55 bar and by higher temperature (330-350°C). At higher hydrogen pressure prefer the hydrodeoxygenation (HDO) reaction (Mikulec et al 2010), the formation of fatty acids and other oxygenated compounds is reduced and therefore high molecular esters are not observed in the reaction products (Guzman et al 2010).

The Liquid Hourly Space Velocity (LHSV) is an important operating parameter for regulating catalyst effectiveness and also catalyst life expectancy (Bezergianni & Kalogianni 2009; Bezergianni et al 2009). The effect of LHSV at five different LHSVs, i.e. 0.5, 1, 1.5, 2 and 2.5 h<sup>-1</sup>. The conversion and product yield of diesel decreasing with increasing LHSV from 0.5 to 2.5 h<sup>-1</sup>. The conversion and overall biofuels yield is favored by decreasing LHSV (at 0.5 h<sup>-1</sup>).

A small percentage of DMDS (di-methyl-di-sulfide) and TBA (tetra-butyl-amine) is added in the feedstock. Heteroatom removal (mainly sulfur, nitrogen and oxygen) is expressed as the percentage of the sulfur (27,200 wppm), nitrogen (219.8 wppm) and oxygen (3.9 wt%) contained in the feed which has been removed during



hydrotreatment reactions at operating temperature 330, 350, 370, 385 and 398°C. As the result, Sulfur and nitrogen is most effectively removed by over 99.4% for all cases. Furthermore, the most difficult element to remove is oxygen. In low temperatures the oxygen removal is low (78.3%). However, by increasing the temperature, the oxygen removal gradually reaches over 99%. it is evident that higher temperatures favor all heteroatom removal from the final products (Bezergianni & Kalogianni 2009); (Bezergianni et al 2010)

### 3.3 Thermodynamic Balance

The studied of thermodynamic model was derived for the total hydrogenation and its predictions were compared with the experimental of rape-seed oil transformation into hydrocarbons. Tristearate was chosen as a model compound to represent vegetable oils in the calculations. As the thermodynamic data for tristearate were not available in literature, their values were estimated by using the Joback's contribution method. Based on the comparison to a relevant known system (butyl stearate) it was concluded that the chosen method is suitable for the assessment of thermodynamic data of triglycerides(Smejkal et al 2009). The Joback's contribution method has been demonstrated to estimate accurately the thermodynamic data of tristearate ( $\Delta H_f = -2176.9$  kJ/mol and  $\Delta G_f = -504.5$  kJ/mol) from Aspen plus. A thermodynamic model for the total hydrogenation of tristearate was derived for temperatures between 250-450 C and hydrogen pressures ranging from 7 to 70 bar. The reaction was assumed to enable isothermal reaction conditions. Phase equilibrium liquid-gas was considered in the model, too (Peng–Robinson and Ideal EOS = Equation of State).The basic reaction mechanism of the proposed catalytic transformation is summarised and consists of two main reactions: hydrodeoxygenation and hydrodecarboxylation, completed by water-gas-shift reaction and CO formation. The thermodynamic balance of the system was used to predict the composition of the liquid phase, namely to predict the distribution of C<sub>17</sub>and C<sub>18</sub> hydrocarbons. The predictions suggest that C<sub>18</sub> hydrocarbons are the main reaction products and that their concentration is affected by temperature and particularly by pressure. Moreover, the model predictions

were found to be in good agreement with experimental data. The estimations suggested that the reaction were limited by hydrogen and triglyceride diffusivity through the liquid film on catalyst particles (Guzman et al 2010).

### 3.4 Catalyst

Catalysts consisting of MO or W supported on  $\gamma$ -alumina carrier with promoters such as Co or Ni are commonly used in the hydrotreating process. Extensive research studies have been devoted over the past decade to developing improved catalysts for the process. Most of studies involve the usage of new or modified support materials, incorporation of additional promoters, modification and optimization of preparation procedures and increase in metal loading. The studies on the activity of catalysts containing both MO and W and promoted by Ni appear to have received little or no attention. The report for the performance of a NiMoW/ $\text{Al}_2\text{O}_3$  catalyst in comparison with conventional NiMo and NiW catalysts for promoting various reactions that occur during to residual oil hydroprocessing. The performance evaluation tests were conducted in a high pressure fixed bed reactor system using vacuum residue as feed. The reactions that were monitored included hydrodesulfurization (HDS) hydrodenitrogenation (HDN), hydrodemetalization (HDM), hydroconversion to distillates (HC). The results revealed that the NiMoW catalyst was more active for various conversions than the NiMo and NiW catalysts. The activity improvement was particularly higher for HDN, HDM, HC reduction. The addition of W to NiMo/ $\text{Al}_2\text{O}_3$  enhanced the hydrogenation function of the catalyst.

Hydrodesulphurization (HDS) of organic molecules as thiophene, benzothiophene and dibenzothiophene (DBT) is generally performed with molybdenum or tungsten sulphides supported on alumina and promoted by Group VIII elements as Cobalt or Nickel with a promoter. Co-promoted catalysts are mainly used for HDS, whereas Ni-promoted catalysts are superior in hydrodenitrogenation (HDN) and hydrogenation (HYD) reactions. Ni-promoted catalysts have not been widely investigated and there is not enough understanding of the nickel-promoting effect (Absi-Halabi et al). The way in which promoter atoms are introduced on the

MoS<sub>2</sub> catalysts, has an influence on the catalytic properties. Cobalt- or nickel promoted unsupported HDS catalysts has been prepared by different methods including, commaceration (Bezergianni et al) and homogeneous sulphide precipitation (Bezergianni et al). Soled et al. (Absi-Halabi et al) have synthesized catalytic trimetallic precursors (Ni–Mo–W). Thus when Mo is substituted at least partially for W, an amorphous phase is produced, whose decomposition and sulphidation produces catalytic active materials. The final products are tested to have enhanced both HDS and HDN activity. On the other hand, with the development of a new catalyst three times more active (NEBULA) (Absi-Halabi et al) than the ones conventionally used in the industry, the research in new and improved catalytic materials for hydrotreatment it has become more important to petroleum industry.

### **3.5 Properties of Production**

Physiochemical properties of the organic liquid products and mixed fuels were determined using standard test procedures designated for diesel fuel or petroleum products. The physical properties of products, which was blend onto mineral diesel fuel in several concentration levels ranging from 5 to 30 wt%. The product obtained by hydroprocessing of rapeseed oil at 360°C and hydrogen pressure of 70 bar was chosen for mixing with diesel fuel from 5 to 30 wt%. As the result, the cetane number increased from 52 (pure mineral diesel) up to 66 (mixed with fuel containing 30 wt%) (Šimáček et al 2010);(Walendziewski et al 2009). On the other hand, the addition of product worsened the low-temperature properties of mixed fuels in comparison with the basic mineral diesel, cloud point and pour point as well as cold filter plugging point (CFPP) were worse. Flash points of mixed fuels were comparable or slightly higher than mineral diesel fuel. It will be necessary to remove light hydrocarbons in order to increase its ignition temperature (Walendziewski et al 2009).

## CHAPTER IV

### EXPERIMENTAL

#### 4.1 Chemicals

Table 4.1 summarizes the details of chemicals used in this experimental studies as well as their suppliers.

4.1.1 Ammonium molybdate hydrate 99.9%  $(\text{NH}_4)_6\text{Mo}_7\text{O}_{27}\cdot 4\text{H}_2\text{O}$  (Sigma Aldrich)

4.1.2 Nickel nitrate hexahydrate 99.9%  $\text{Ni}(\text{NO}_3)_2\cdot 6\text{H}_2\text{O}$  (Sigma Aldrich)

4.1.3 Cobalt nitrate hexahydrate 99.9%  $\text{Co}(\text{NO}_3)_2\cdot 6\text{H}_2\text{O}$  (Sigma Aldrich)

4.1.4 Ammonium paratungstate heptahydrate 99.9%  $\text{H}_{40}\text{N}_{10}\text{O}_{41}\cdot 7\text{H}_2\text{O}$  (Fluka)

4.1.5 Palmitic acid (Sigma Aldrich)

4.1.6 Stearic acid (Sigma Aldrich)

4.1.7 Oleic acid (Sigma Aldrich)

4.1.8 Hydrogen  $\text{H}_2$  UHP (Linde)

4.1.9 Helium UHP (Linde)

4.1.10 Methane (Linde)

4.1.11 Oxygen HP (Linde)

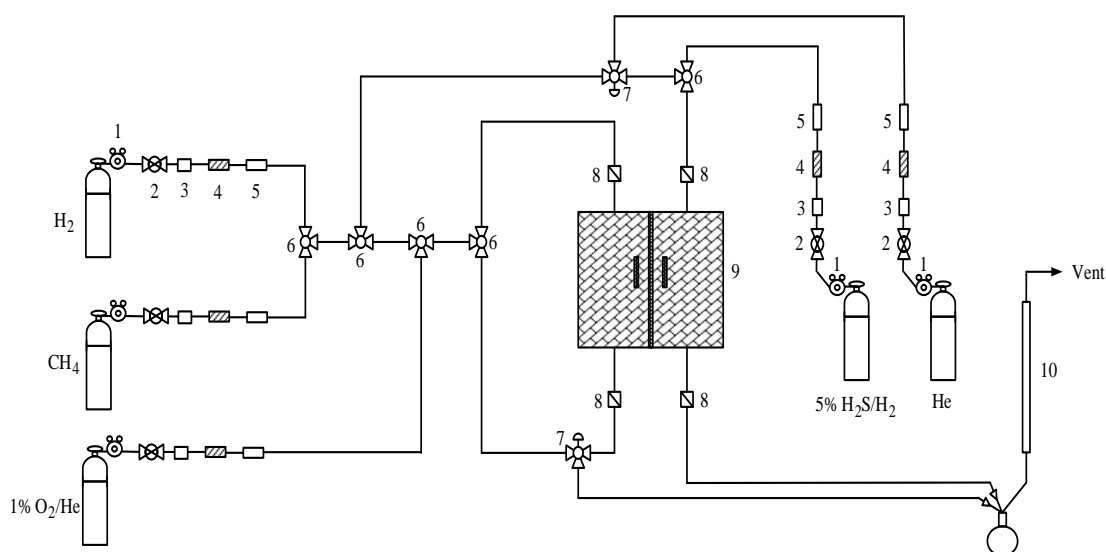
4.1.12 Aluminium oxide (Sigma Aldrich)

## 4.2 Catalysts Preparation

### 4.2.1 Preparation of NiMo-NiMoW/Al<sub>2</sub>O<sub>3</sub> and CoMo-CoMoW/ Al<sub>2</sub>O<sub>3</sub>

NiMo/Al<sub>2</sub>O<sub>3</sub> and CoMo/Al<sub>2</sub>O<sub>3</sub> were prepared from nickel nitrate hexahydrate 99.9% Ni(NO<sub>3</sub>)<sub>2</sub>·6H<sub>2</sub>O, cobalt nitrate hexahydrate 99.9% Co(NO<sub>3</sub>)<sub>2</sub>·6H<sub>2</sub>O, ammonium molybdate hydrate 99.9% (NH<sub>4</sub>)<sub>6</sub>Mo<sub>7</sub>O<sub>27</sub>·4H<sub>2</sub>O and ammonium paratungstate heptahydrate as precursors. Al<sub>2</sub>O<sub>3</sub> was used as support. Catalysts were synthesized using incipient wetness impregnation method. Bimetallic catalysts were prepared in three steps with intermediate drying of 40% (first step), 35% (second step), and 25% (third step) of the precursor liquid dropped on Al<sub>2</sub>O<sub>3</sub>. The obtained catalysts were dried at 110°C for 24 hr and then calcined at 500°C for 5 hr. Ammonium paratungstate heptahydrate was dissolved in distilled water and dropped on NiMo/Al<sub>2</sub>O<sub>3</sub> or CoMo/Al<sub>2</sub>O<sub>3</sub> calcined catalyst. Catalyst was dried at 110°C for 24 hr and then calcined at 500°C for 3 hr to obtain NiMoW/Al<sub>2</sub>O<sub>3</sub> or CoMoW/Al<sub>2</sub>O<sub>3</sub> catalyst.

The supported oxycarbide catalysts were prepared by passing a 20% CH<sub>4</sub>/H<sub>2</sub> (v/v) gas mixture over approximately 0.2 g of the solid precursor. The synthesis was carried out in a tubular reactor of 8 mm o.d. (6 mm i.d.) placed in a furnace controlled by a temperature programmer. First the sample was heated to 400°C at a heating rate of 3°C/min with flowing He (flow rate = 50 cm<sup>3</sup>/min). At this temperature, the flow was switched to 20% CH<sub>4</sub>/H<sub>2</sub> (v/v) gas mixture at a flow rate of 50 cm<sup>3</sup>/min, and then the temperature was ramped at a heating rate of 1°C/min from 400 to 700°C. The carburization of the sample was monitored by analyzing the consumption of methane and the formation of CO and CO<sub>2</sub> using gas chromatography with thermal conductivity detector (GC-8A). The 20% CH<sub>4</sub>/H<sub>2</sub> (v/v) gas mixture passed through the sample until no CO<sub>2</sub> were detected in the exhausted gas. Then the gas flow was switched from CH<sub>4</sub>/H<sub>2</sub> to He for cooling down the sample to room temperature. After that the system was switched to a gas mixture containing 1% O<sub>2</sub> in He (v/v) stream for 16 h to form a protective oxide layer that prevented bulk oxidation. Before being used in reaction, catalysts were reduced at 400°C in H<sub>2</sub> flow for 2 hour to remove the protective oxide layer. (Schwartz et al 2000)



- |                       |                   |               |
|-----------------------|-------------------|---------------|
| 1. Pressure Regulator | 2. On-Off Valve   | 3. Gas Filter |
| 4. Mass Flow Meter    | 5. Check Valve    | 6. 3-way      |
| 7. 3-way Valve        | 8. Sampling point | 9. Furnace    |
| 10. Bubble Flow Meter |                   |               |

**Figure 4.1** Show the flow diagram of synthesis metal carbides and presulfided catalysts

### 4.3 Catalyst Characterization

#### 4.3.1 X-ray Diffraction (XRD)

XRD measurement was performed to determine the bulk phase of catalysts by SIEMENS D 5000 X-ray diffractometer connected with a computer with Diffract ZT version 3.3 programs for fully control of the XRD analyzer. The experiments were carried out by using  $\text{CuK}\alpha$  radiation with Ni filter in the  $2\theta$  range of 20–80 degrees resolution  $0.02^\circ$ . The crystallite size was estimated from line broadening according to the Scherrer's equation, and  $\alpha\text{-Al}_2\text{O}_3$  was used as standard.

X-ray diffraction (XRD) was used for catalyst characterization. The XRD patterns were obtained using a D8 Advance of Bruker AXS, equipped with a long fine

focus ceramic Cu K $\alpha$  X-ray source. The pattern was recorded in the range of  $20^\circ < 2\theta < 80^\circ$  with incremental steps of  $0.04^\circ$ , and a scan speed of 0.5 s/step.

### 4.3.2 Nitrogen Physisorption (BET)

BET apparatus for the single point method: the reaction apparatus of BET surface area measurement consisted of two feed lines for helium and nitrogen. The flow rate of the gas was adjusted by means of a fine-metering valve on the gas chromatography. The sample cell was made of pyrex glass. The mixture gases of helium and nitrogen flew through the system at the nitrogen relative of 0.3. The catalyst sample (ca. 0.05 g) was placed in the sample cell, which was then heated up to  $150^\circ\text{C}$  and hold at this temperature for 3 hours. After that the catalyst sample was cooled down to room temperature and nitrogen uptakes were measured as follows.

4.4.2.1 Adsorption step: The sample set in the sample cell was dipped into liquid nitrogen. Nitrogen gas would be adsorbed on the surface of the sample until equilibrium was reached.

4.4.2.2 Desorption step: The sample cell with nitrogen gas-adsorption catalyst sample was dipped into water at room temperature. The adsorbed nitrogen gas was desorbed from the surface of the sample. This step was completed when the indicator line was at the position of base line.

4.4.2.3 Calibration step: 1 ml of nitrogen gas at atmospheric pressure was injected through the calibration port of the gas chromatography and the area was measured. The area represented the calibration peak.

The surface areas of the catalyst and adsorbent were obtained from  $\text{N}_2$  adsorption and desorption BET isotherms using a Micromeritics Chemisorp 2750. The nitrogen adsorption desorption isotherms were obtained at  $-196^\circ\text{C}$  with 0.1 g of catalyst.

### **4.3.3 H<sub>2</sub> Temperature Programmed Reduction (H<sub>2</sub>-TPR)**

H<sub>2</sub>-TPR was used to determine the reduction behaviors of the samples using a Micrometric Chemisorb 2750.

4.4.3.1 The catalyst sample of 0.05 g was loaded in the sample cell.

4.4.3.2 Prior to operation, the catalyst was heated up to 150°C in flowing nitrogen and held at this temperature for 1 hour.

4.4.3.3 After that the catalyst sample was cooled down to room temperature under nitrogen flow, the carrier gas of 5% H<sub>2</sub> in Ar (30 CC/min) were ramped from 35 to 800°C at a rate of 10°C/min.

4.4.3.4 A cold trap was placed before the detector to remove water produced during the reaction.

4.4.3.5 A thermal conductivity detector (TCD) was used to determine the amount of hydrogen consumption during TPR.

### **4.3.4 Inductively Coupled Plasma-Optical Emission Spectroscopy (ICP-OES)**

Element analysis by Inductively Coupled Plasma-Optical Emission Spectroscopy (ICP-OES) was used to determine composition in catalysts. The instrument used for the measurement was Perkin Elmer 20 model PLASMA-1000. Approximately, 0.03 g of catalyst was dissolved in 5 ml of 49% hydrofluoric acid. The sample was stirred at 60°C until the sample was completely dissolved. Then solution was dilute to 100 ml with deionized water.



#### **4.3.5 Ammonia Temperature Program Desorption (NH<sub>3</sub>-TPD)**

The temperature program desorption (TPD) using NH<sub>3</sub> gas as an adsorbed probe molecule was performed in BELCAT-A. Approximately, 0.05g of catalyst was introduced to glass tube in temperature control furnace. Then helium gas at a flow rate of 25 ml/min was fed through the catalyst and then heated up to 500°C with a ramping rate of 10°C/min and held for 1 hour to remove moisture. After that it was cooled down to 40°C and fed by 10%NH<sub>3</sub>/He for 30 minutes and He for 45 minutes. Finally it was heated up to 500°C with a ramp rate of 10°/min to desorb NH<sub>3</sub> which was detected by TCD detector and recorded by computer.

## **CHAPTER V**

### **RESULTS AND DISCUSSION**

This chapter presents the results of reaction tests and the catalyst characterization from the study on hydroprocessing process for biodiesel production. The reaction performances were reported in terms of conversion, selectivity and product yield.

#### **5.1 Catalyst Characterization**

In this section, the characteristics of NiMo, NiMoW, CoMo and CoMoW were investigated by mean of various techniques such as N<sub>2</sub>-physisorption, Inductively Coupled Plasma-Optical Emission Spectroscopy, X-ray Diffraction, H<sub>2</sub> Temperature Program Reduction (H<sub>2</sub>-TPR), Ammonia Temperature Programmed Desorption (NH<sub>3</sub>-TPD).

##### **5.1.1 Inductively Coupled Plasma-Optical Emission Spectroscopy (ICP-OES)**

In order to confirm the composition of Ni, Co, Mo and W loading on the catalyst from the preparation step by impregnation method, this technique was necessary to apply as shown the result in Table 5.1. The percent of metal loading from the commercial catalysts were 2.45 wt.% of Nickel (Ni) and 9.4 wt.% Molybdenum (Mo) for NiMo catalyst, 2.54 wt.% Cobalt (Co) and 9.71 wt.% Molybdenum (Mo) for CoMo catalyst and 6 wt.% of Tungsten (W). From this result, the metal loadings on the catalyst were in the range of acceptable value.

**Table 5.1** The element composition determining by ICP-OES

Catalysts	Composition (wt.%)			
	Ni	Co	W	Mo
NiMo	2.71	-	-	10.05
NiMoW	2.5	-	6.20	9.17
CoMo	-	2.46	-	9.28
CoMoW	-	2.63	5.42	9.80

### 5.1.2 N<sub>2</sub> Physisorption

This section discusses the surface area, pore volume and pore size of the catalysts with nitrogen gas at -196°C for determining the physical properties of catalysts. The results from this technique are shown in Table 5.2

**Table 5.2** Surface area, pore volume, and pore size of catalysts obtain from N<sub>2</sub> physisorption method

Catalysts	Surface area (m <sup>2</sup> /g)	Pore volume (cm <sup>3</sup> /g)	Pore size (nm)
Support Al <sub>2</sub> O <sub>3</sub>	145.44	0.21	5.92
NiMo	118.35	0.14	4.91
NiMoW	97.92	0.13	5.54
CoMo	113.5	0.16	5.86
CoMoW	101.17	0.14	5.83

From this table, after impregnating the metal the surface area of support was decreased. The tungsten loading on catalysts also affected the surface area of the catalyst. The pore volume and pore size of the support decreased similar to the tendency of surface area.

### 5.1.3 X-ray Diffraction

The phases of catalysts after impregnation of metal to support were determined by XRD measurement.

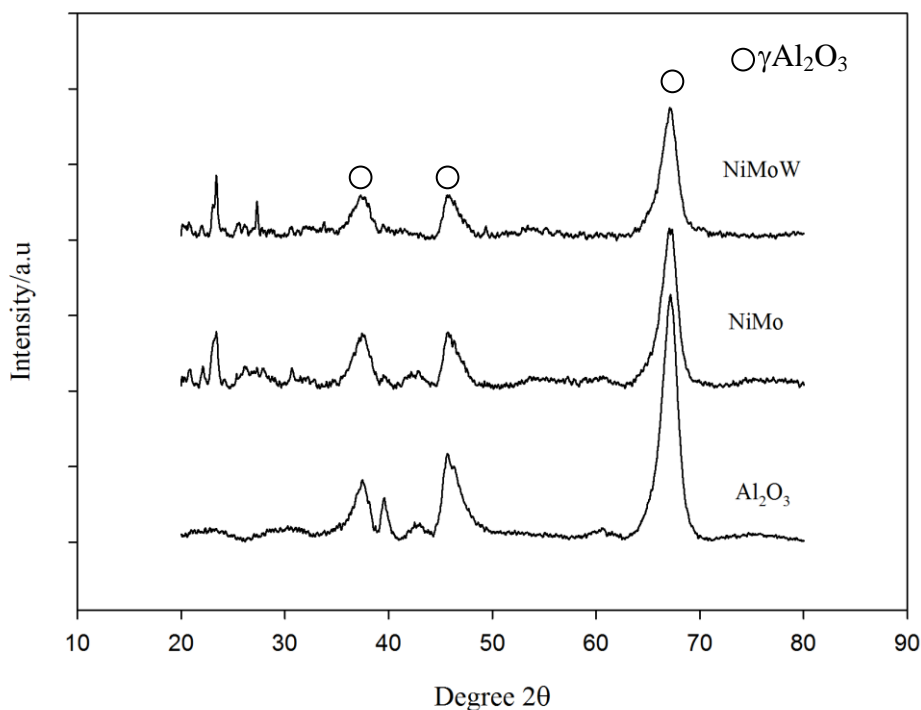


**Figure 5.1** XRD patterns of NiMo/Al<sub>2</sub>O<sub>3</sub> and NiMoW/Al<sub>2</sub>O<sub>3</sub> catalysts

The important phases of the catalysts were  $\gamma$ -Al<sub>2</sub>O<sub>3</sub>, NiO, Co<sub>3</sub>O<sub>4</sub>, NiMoO<sub>4</sub>, CoMoO<sub>4</sub>, MoO<sub>4</sub> and WO<sub>3</sub>. The XRD spectra of  $\gamma$ -Al<sub>2</sub>O<sub>3</sub> support, NiMoW/ $\gamma$ -Al<sub>2</sub>O<sub>3</sub>, NiMo/ $\gamma$ -Al<sub>2</sub>O<sub>3</sub>, CoMoW/ $\gamma$ -Al<sub>2</sub>O<sub>3</sub> and CoMo/ $\gamma$ -Al<sub>2</sub>O<sub>3</sub> catalysts are shown in Figures 5.1 and 5.2. Peaks at 38°, 46° and 67° for  $\gamma$ -Al<sub>2</sub>O<sub>3</sub> appear in all catalysts. Considering Figure 5.1, the peak at 26.56° was assigned to NiMoO<sub>4</sub> while those at 27°, 34°, 49°, 53°, and 55° were attributed to molybdenum oxide (MoO<sub>4</sub>) (Rojanapipatkul &

Jongsomjit 2008). The XRD patterns of NiMoW/ $\gamma$ -Al<sub>2</sub>O<sub>3</sub> catalysts contained low peak intensity at 14°. As displayed in Figure 5.2, the peak at 26.48° represented CoMoO<sub>4</sub> while at 31°, 37°, 45°, 59° and 65° represent cobalt oxide (Co<sub>3</sub>O<sub>4</sub>) and low peak intensities at 25°, 28°, 32.5°, and 38° for CoMoW/ $\gamma$ -Al<sub>2</sub>O<sub>3</sub> catalysts were observed (Huirache-Acuña et al 2009).

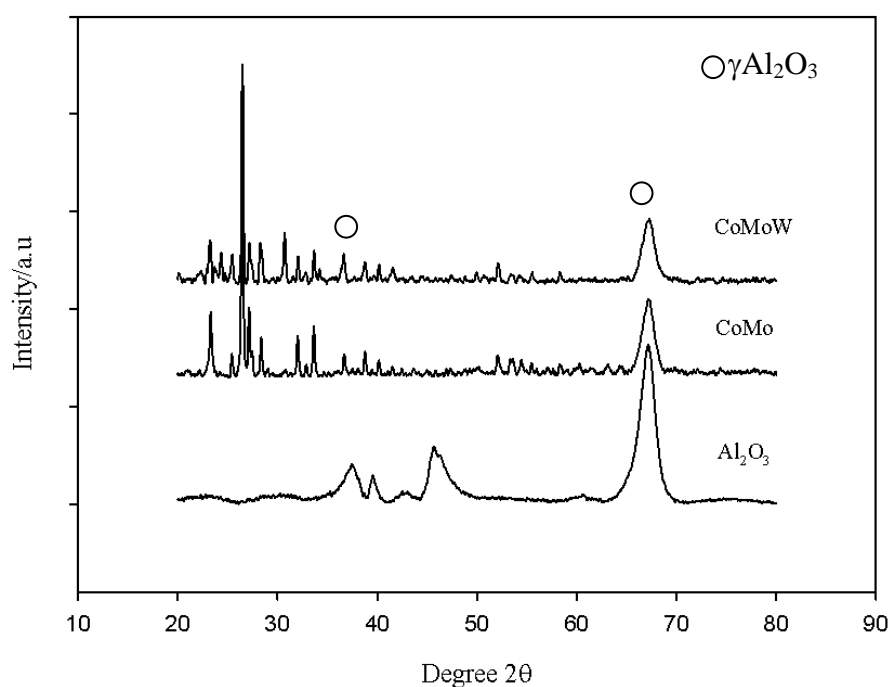


**Figure 5.2** XRD patterns of NiMo/Al<sub>2</sub>O<sub>3</sub> and NiMoW/Al<sub>2</sub>O<sub>3</sub>

#### 5.1.4 H<sub>2</sub> Temperature-Programmed Reduction (H<sub>2</sub>-TPR)

The temperature-programmed reduction with H<sub>2</sub> (H<sub>2</sub>-TPR) was performed in order to investigate the reducibility of the catalyst by reducing an oxide form to a metal form. The interaction of metal and support could be obtained from the TPR experiments. The results as shown in Figures 5.3 and 5.4 indicated the reduction behavior of the catalysts with the effect of the alumina support. The reduction is an important step in carbidation of the catalysts for converting to the active form before carrying out the hydroprocessing process.

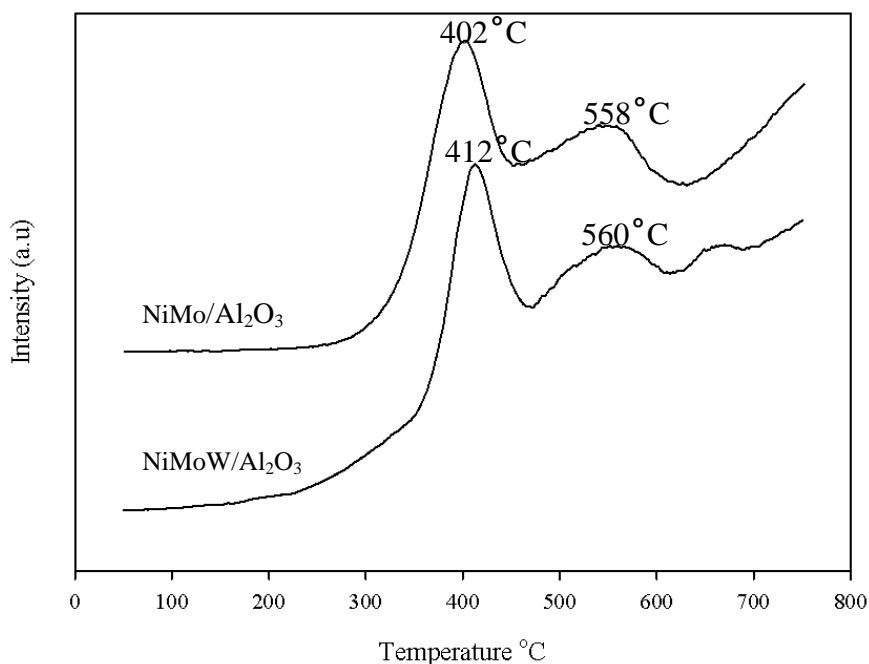


**Figure 5.3** H<sub>2</sub>-TPR of NiMo/Al<sub>2</sub>O<sub>3</sub> and NiMoW/Al<sub>2</sub>O<sub>3</sub>

Figure 5.3 shows the reduction profile of the NiMo/Al<sub>2</sub>O<sub>3</sub> and NiMoW/Al<sub>2</sub>O<sub>3</sub> catalysts while those of CoMo and CoMoW catalysts are illustrated in Figure 5.4. For NiMo and NiMoW catalysts, the reduction in temperature of the catalysts were observed at 402°C and 558 °C for NiMo and 412°C and 560°C for NiMoW. In Figure 5.4 shows the reduction profiles of CoMo and CoMoW catalysts, the reduction temperature were observed at 447°C and 580°C for CoMo and 464°C and 591°C for CoMoW catalysts, depending on metal in the catalysts. For the first peak, it was ascribed to the reduction of Mo<sup>6+</sup> (MoO<sub>3</sub>) to Mo<sup>4+</sup> (MoO<sub>2</sub> and/or CoMoO<sub>4</sub> and NiMoO<sub>4</sub>). For the addition of tungsten on the catalyst, it was found that the reduction temperature is increased for both NiMo and CoMo catalysts.

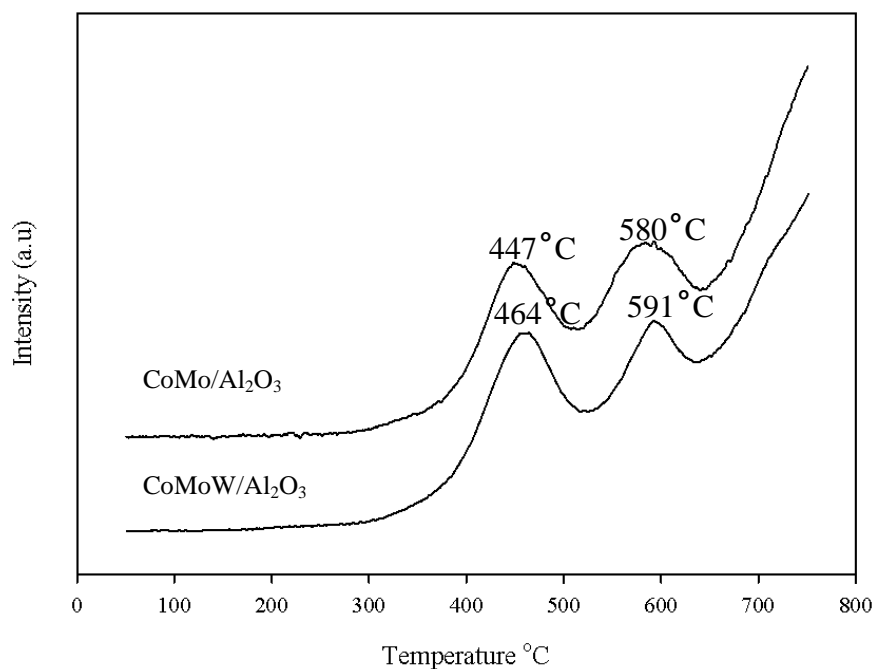


**Figure 5.4** H<sub>2</sub>TPR of CoMo/Al<sub>2</sub>O<sub>3</sub> and CoMoW/Al<sub>2</sub>O<sub>3</sub>

### 5.1.5 Ammonia Temperature Programmed Desorption (NH<sub>3</sub>-TPD)

This technique explains the detail about surface acidity by using NH<sub>3</sub> as probe molecule in order to determine the acidity on the catalyst surface in qualitative and quantitative forms. The results are shown in Figure 5.5 for NiMo/Al<sub>2</sub>O<sub>3</sub> and NiMoW/Al<sub>2</sub>O<sub>3</sub> catalyst and Figure 5.6 for CoMo/Al<sub>2</sub>O<sub>3</sub> and CoMoW/Al<sub>2</sub>O<sub>3</sub> catalysts.

According to Figures 5.5 and 5.6 it was revealed that the addition of tungsten to NiMo and CoMo catalysts can shift the peak to higher temperature because tungsten has the interaction with NH<sub>3</sub> more than NiMo and CoMo catalysts. Therefore, tungsten in the catalysts could exhibit higher acid site strength than NiMo and CoMo catalysts

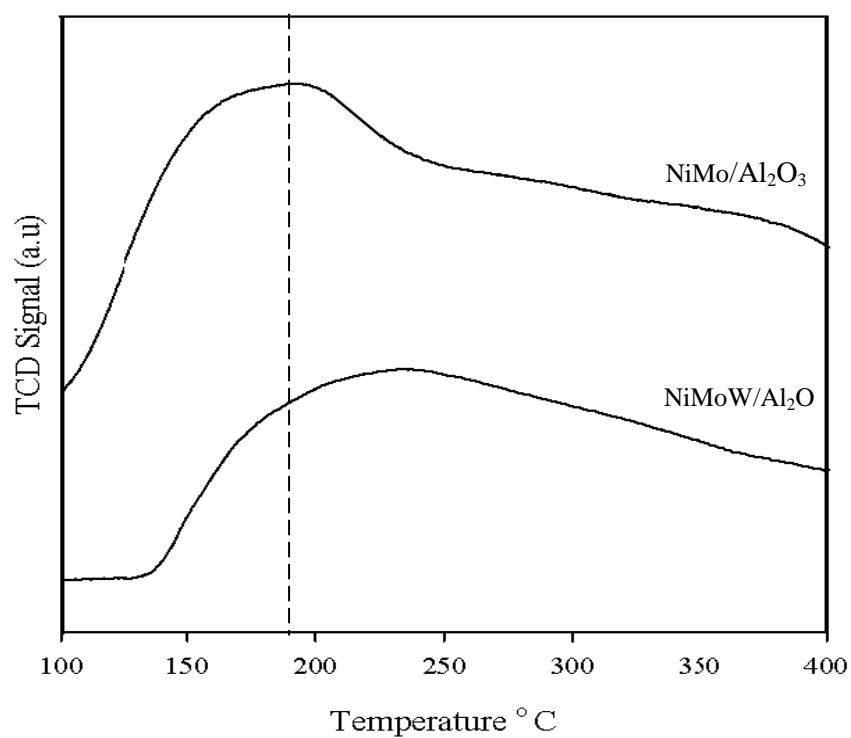


**Figure 5.5** NH<sub>3</sub>TPD profile of NiMo/Al<sub>2</sub>O<sub>3</sub> and NiMoW/Al<sub>2</sub>O<sub>3</sub> catalysts

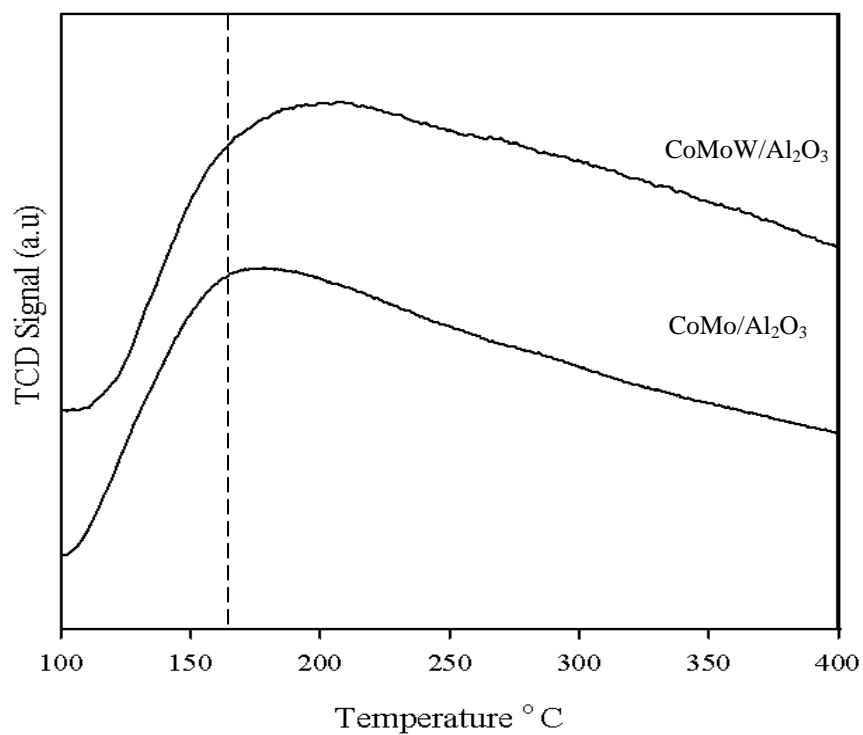


**Figure 5.6** NH<sub>3</sub>TPD profiles of CoMo/Al<sub>2</sub>O<sub>3</sub> and CoMoW/Al<sub>2</sub>O<sub>3</sub>



## 5.2 Hydrotreated Hydrogenation of Fatty Acid

For the hydroprocessing process there were three main reaction i.e. hydrodeoxygenation, decarboxylation and decarbonylation that occurred in order to remove the oxygen atom in carbonyl group of fatty acid molecule. As considered the studied fatty acids i.e. oleic acid, stearic acid and palmitic acid, the related reactions in hydroprocessing process were listed in the following reactions [reaction (5.1-5.10)]

### For Oleic acid (C18:1)

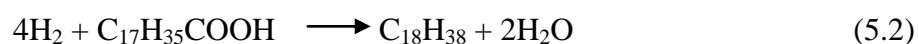
1<sup>st</sup> step

Hydrogenation

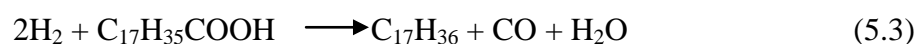


2<sup>nd</sup> step

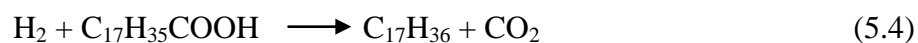
Hydrodeoxygenation



Decarbonylation

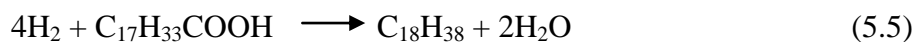


Decarboxilation

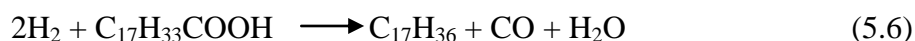


For Stearic acid(C18:0)

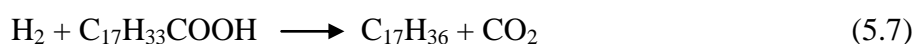
Hydrodeoxygenation



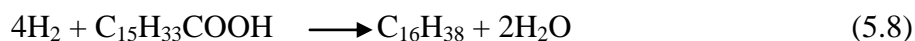
Decarbonylation



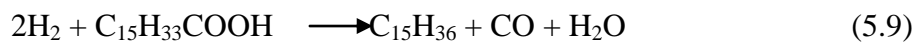
Decarboxylation

For Palmitic acid (C16:0)

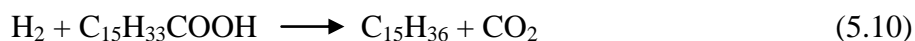
Hydrodeoxygenation



Decarbonylation



Decarboxylation



Regarding the reaction performances, it was studied in term of conversion, selectivity and product yield as expressed in the following equations.

$$\text{Conversion} = \frac{(\text{weight of fatty acid})_{\text{in feed}} - (\text{weight of fatty acid})_{\text{in product}}}{(\text{weight of fatty acid})_{\text{in feed}}} \times 100 \quad (5.11)$$

$$\text{Selectivity} = \frac{\% \text{ Alkane } \text{C}_{15} - \text{C}_{18}}{\% \text{ Total Alkane}} \times 100 \quad (5.12)$$

$$\text{Diesel yield} = \frac{\text{Conversion} \times \text{Selectivity}}{100} \quad (5.13)$$

### 5.2.1 Effect of Temperature and Reaction time on Conversion and Diesel Yield

#### Oleic acid (C18:1)

The effects of temperature and reaction time from the process with CoMo and CoMoW catalysts on the conversion are provided in Figures 5.7 and 5.8. It showed that the conversion increases with increasing the temperature and reaction time. In addition the maximum conversion of 97% was achieved. For CoMo and CoMoW catalysts slight increase in conversion was obtained at longer reaction time, whrer the conversion for NiMo and NiMoW catalysts apparently increased with increasing temperature at short reaction time as illustrated in Figures 5.9 and 5.10 compared to the results from other fatty acids as further shown in Figure 5.11-5.18, the conversion of oleic acid obtain from CoMo and CoMoW catalysts closed to 100% because the double bond in oleic acid molecule was hydrogenated easier. However, the oleic acid conversion at low temperature was higher than the stearic acid and palmitic acid conversion. In term of diesel yield, its increase in was gained, when the temperature increased, while it reduced at longer operating reaction time. From the CoMo catalyst with adding tungsten the odd number of carbon was yield less than the even number of carbon atoms.

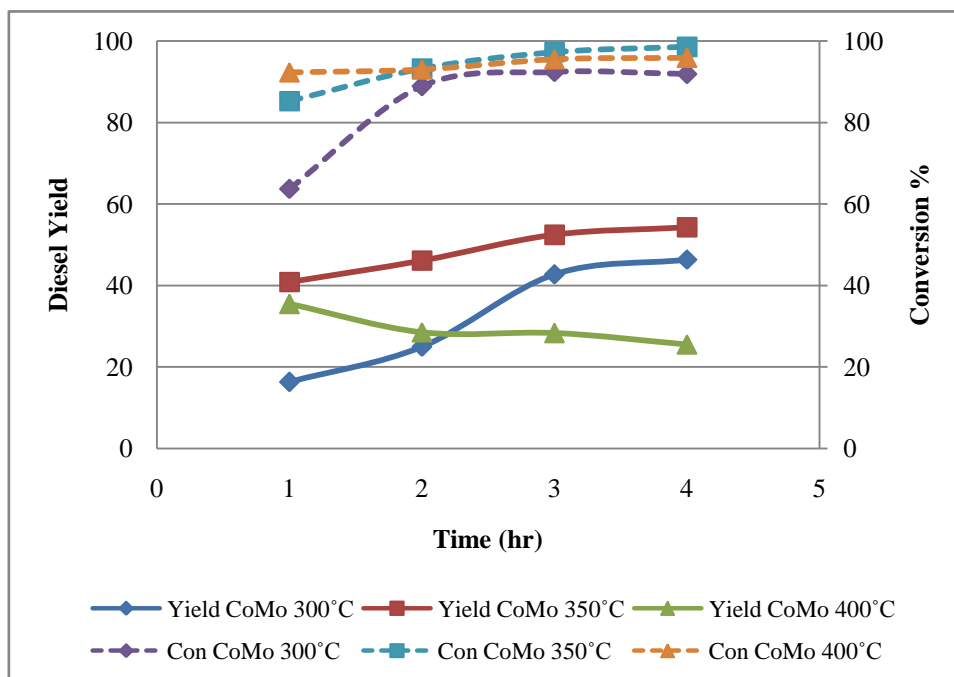


**Figure 5.7** Conversion of oleic acid and diesel yield obtain from CoMo/ $\gamma$ Al<sub>2</sub>O<sub>3</sub> catalyst under H<sub>2</sub> pressure of 40 bar

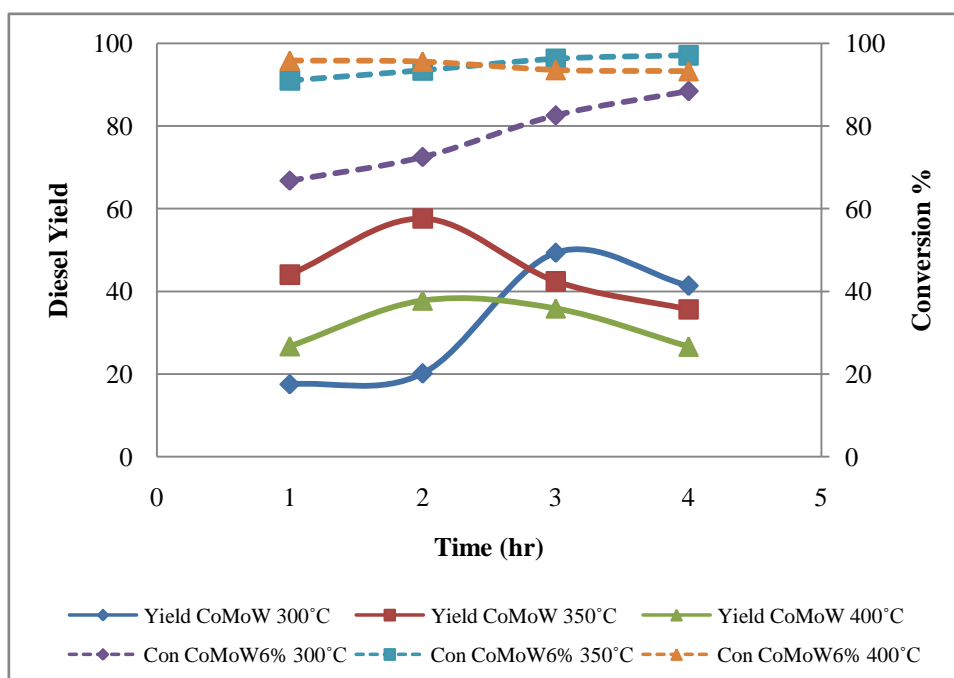


**Figure 5.8** Conversion of oleic acid and diesel yield obtain from CoMoW/ $\gamma$ Al<sub>2</sub>O<sub>3</sub> catalyst under H<sub>2</sub> pressure of 40 bar

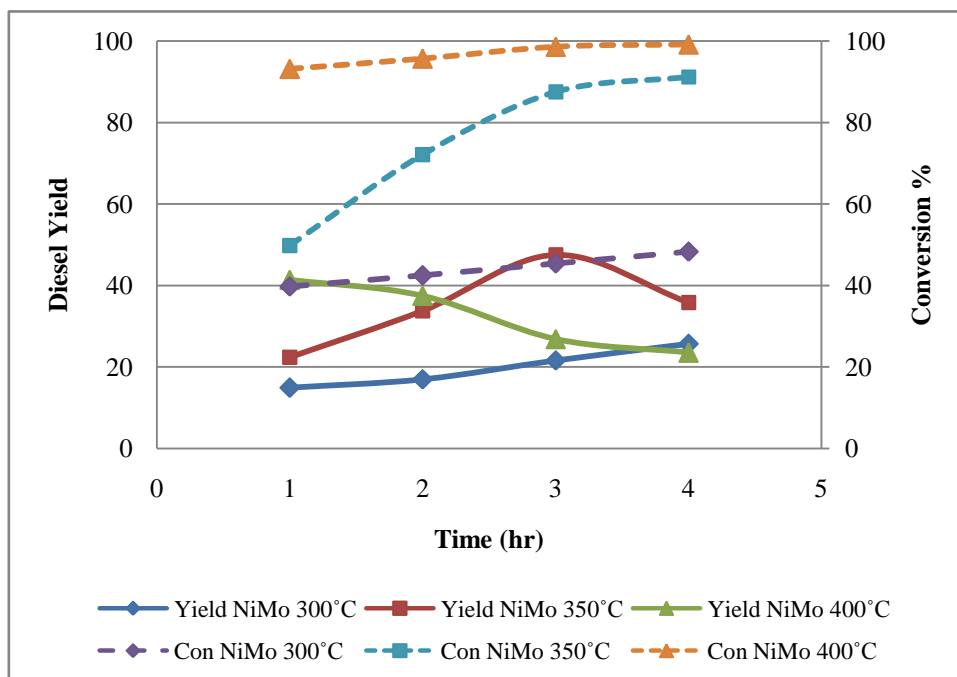


**Figure 5.9** Conversion of oleic acid and diesel yield obtain from NiMo/ $\gamma$ Al<sub>2</sub>O<sub>3</sub> catalyst under H<sub>2</sub> pressure of 40 bar

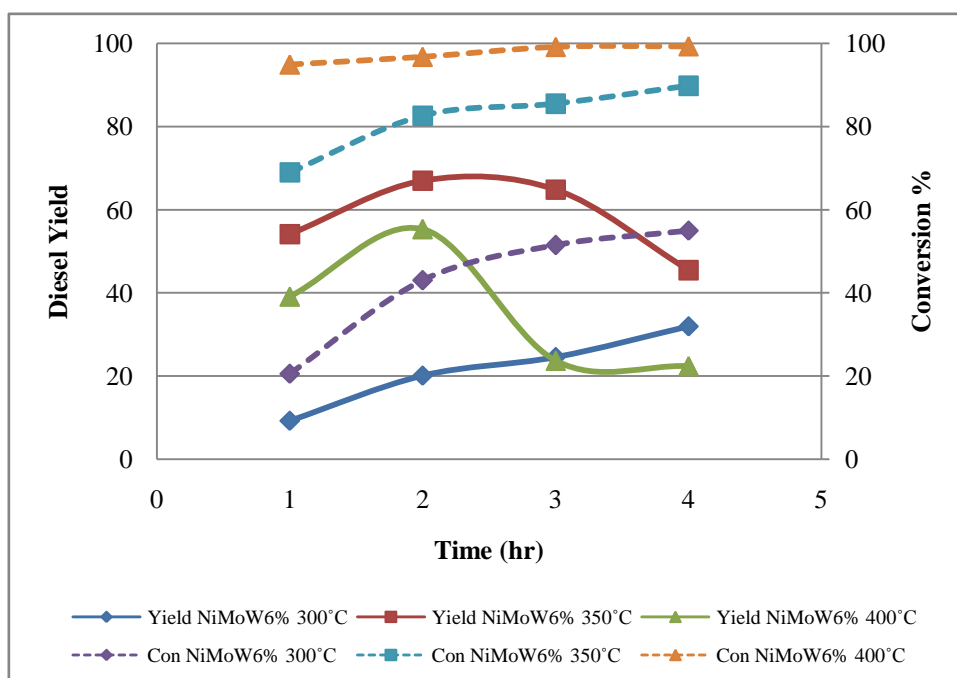


**Figure 5.10** Conversion of oleic acid and diesel yield obtain from NiMoW/ $\gamma$ Al<sub>2</sub>O<sub>3</sub> catalyst under H<sub>2</sub> pressure of 40 bar

Stearic acid (C18:0)

Considering the effect of temperature on the conversion of stearic acid small effect was appeared when the operating condition was at low temperature; however, it was more pronounced at higher temperature. As known, the absence of a double bond in stearic acid molecule is existed. Therefore the hydrogenation step was not taken into account, resulting in the conversion of stearic acid was lower than that of oleic acid. The CoMoW catalyst exhibit higher effect on the conversion than the CoMo catalyst As shown in Figure 5.12 in case of 400°C the conversion was nearly 100% at 2 hour of reaction time. Nonetheless, longer reaction time was required for NiMo and NiMoW catalysts in order to achieve the conversion approximately 100%. For all studied catalysts yield and selectivity at the temperature 400°C dropped with processing long reaction time. It could be presumed that occurrence of the strong adsorption of carbonaceous ppecies on the catalyst surface and cracking reaction in the system for low and high temperature case, respectively, causes the presence of their peak. The conversion selectivity and diesel yield of stearic acid (C<sub>15</sub>-C<sub>18</sub>) calculate from equation 5.11-5.13

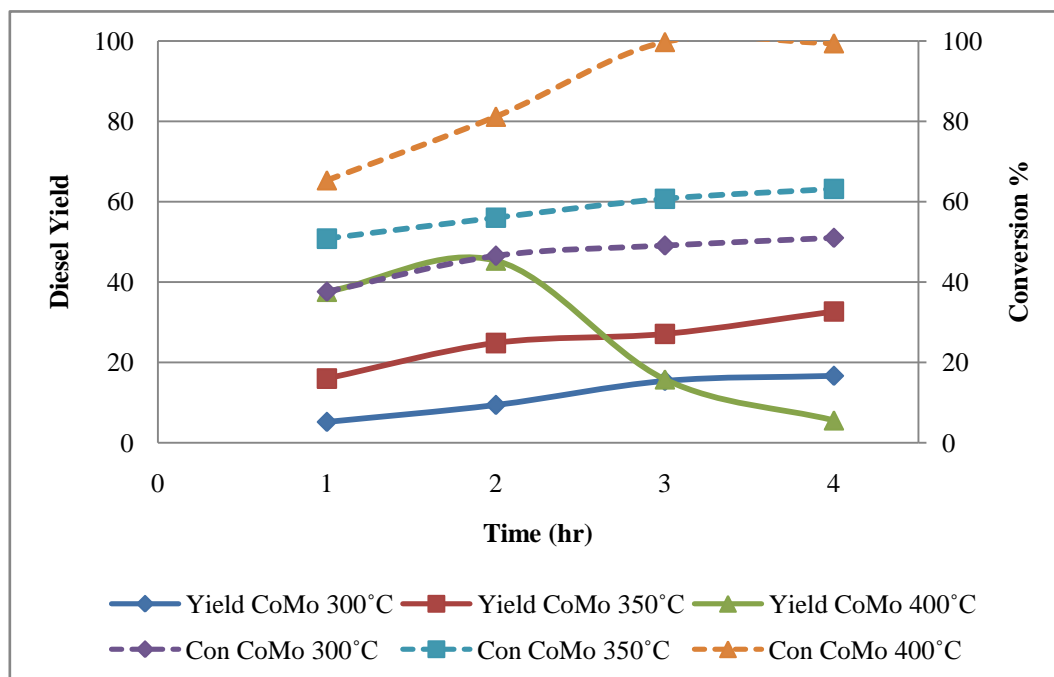


**Figure 5.11** Conversion of stearic acid and diesel yield obtain from CoMo/ $\gamma$ Al<sub>2</sub>O<sub>3</sub> catalyst under hydrogen pressure 40 bar

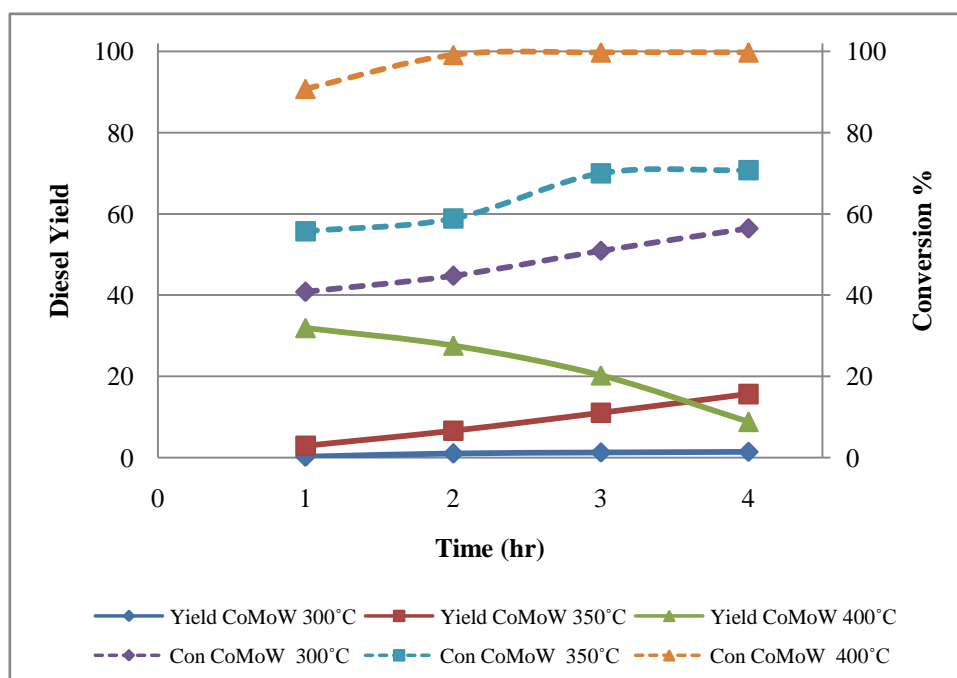


**Figure 5.12** Conversion of stearic acid and diesel yield obtain from CoMoW/ $\gamma$ Al<sub>2</sub>O<sub>3</sub> catalyst under hydrogen pressure 40 bar

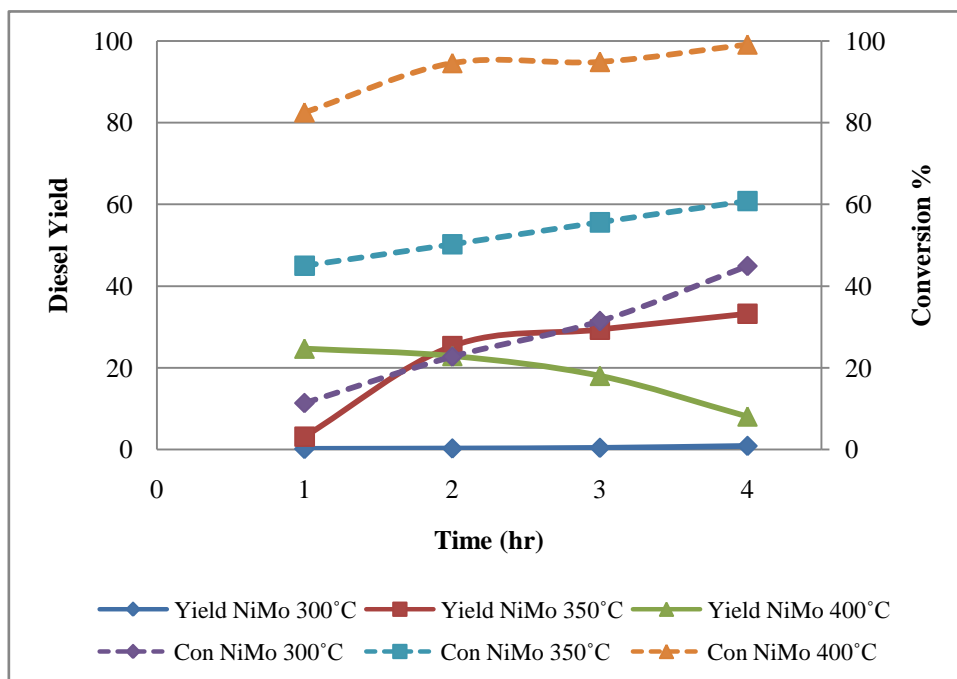


**Figure 5.13** Conversion of stearic acid and diesel yield obtain from NiMo/ $\gamma$ Al<sub>2</sub>O<sub>3</sub> catalyst under hydrogen pressure 40 bar

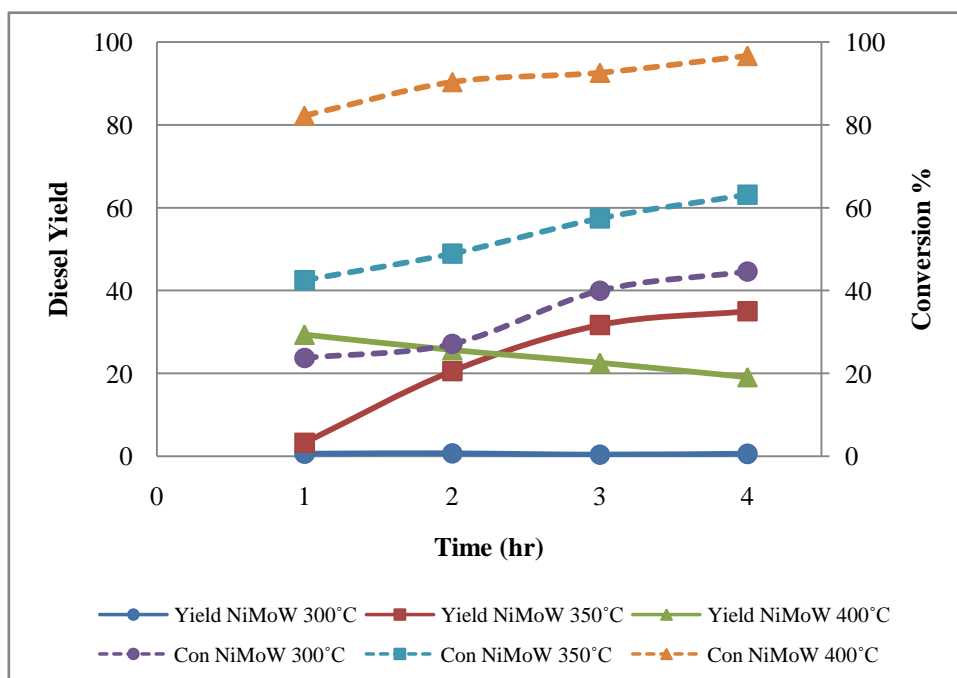


**Figure 5.14** Conversion of stearic acid and diesel yield obtain from NiMoW/ $\gamma$ Al<sub>2</sub>O<sub>3</sub> catalyst under hydrogen pressure 40 bar



Palmitic acid (C16:0)

The effect of temperature on the conversion and diesel yield of palmitic acid was investigated as shown in Figures 5.15-5.18. It was found that the conversion of palmitic acid and diesel yield at the temperature of 300 and 350 °C were very low for all of catalysts similar to stearic acid. Compared to CoMo and CoMoW catalysts, both of NiMo and NiMoW catalysts exhibited higher conversion at reaction time 1 h. The molecule of palmitic acid consists of carbon sixteen atom atom without a double bond . At 400°C, the diesel yield from hydroprocessing process of palmitic acid was higher than that of stearic acid process because the chain of palmitic acid (C16:0) is shorter than that of stearic acid (C18:0). The long chain molecule was hardly to adsorbed on catalyst surface as a result of the catalyst surface require for long chain molecule, compared to short one

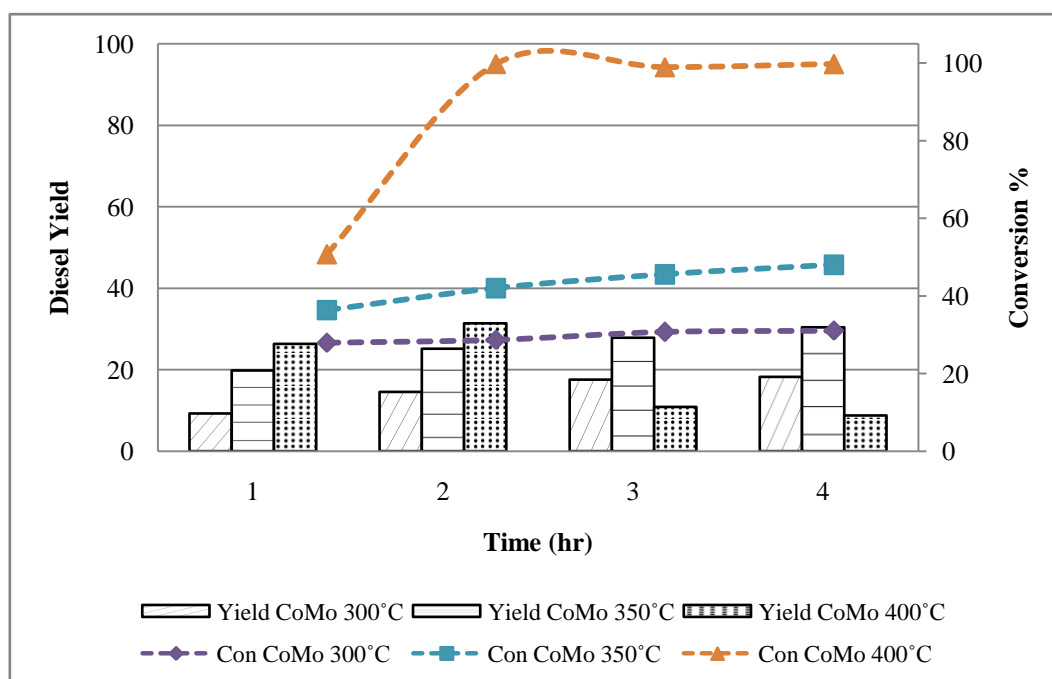


**Figure 5.15** Conversion of palmitic acid and diesel yield obtain from CoMo/ $\gamma$ Al<sub>2</sub>O<sub>3</sub> catalyst under hydrogen pressure 40 bar

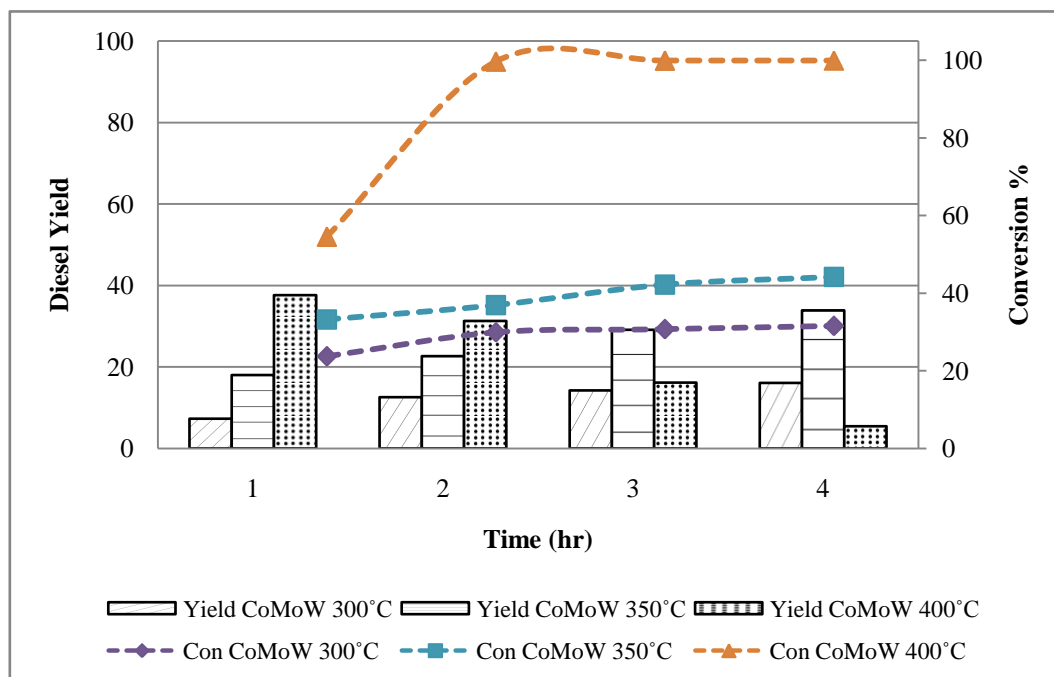


**Figure 5.16** Conversion of palmitic acid and diesel yield obtain from CoMoW/ $\gamma$ Al<sub>2</sub>O<sub>3</sub> catalyst under hydrogen pressure 40 bar

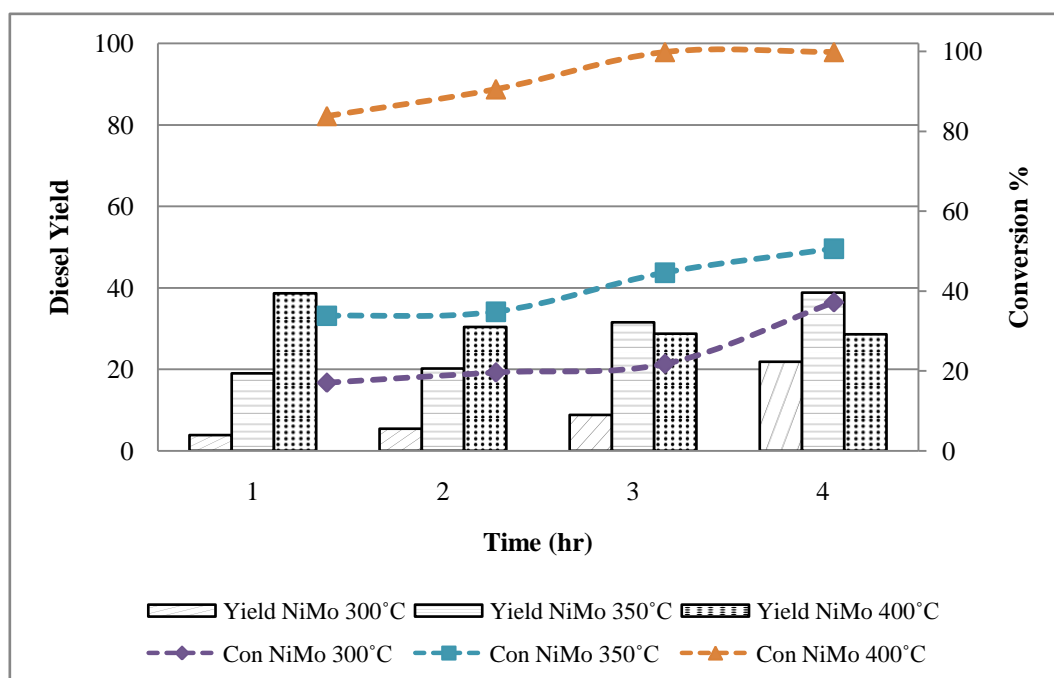


**Figure 5.17** Conversion of palmitic acid and diesel yield obtain from NiMo/ $\gamma$ Al<sub>2</sub>O<sub>3</sub> catalyst under hydrogen pressure 40 bar

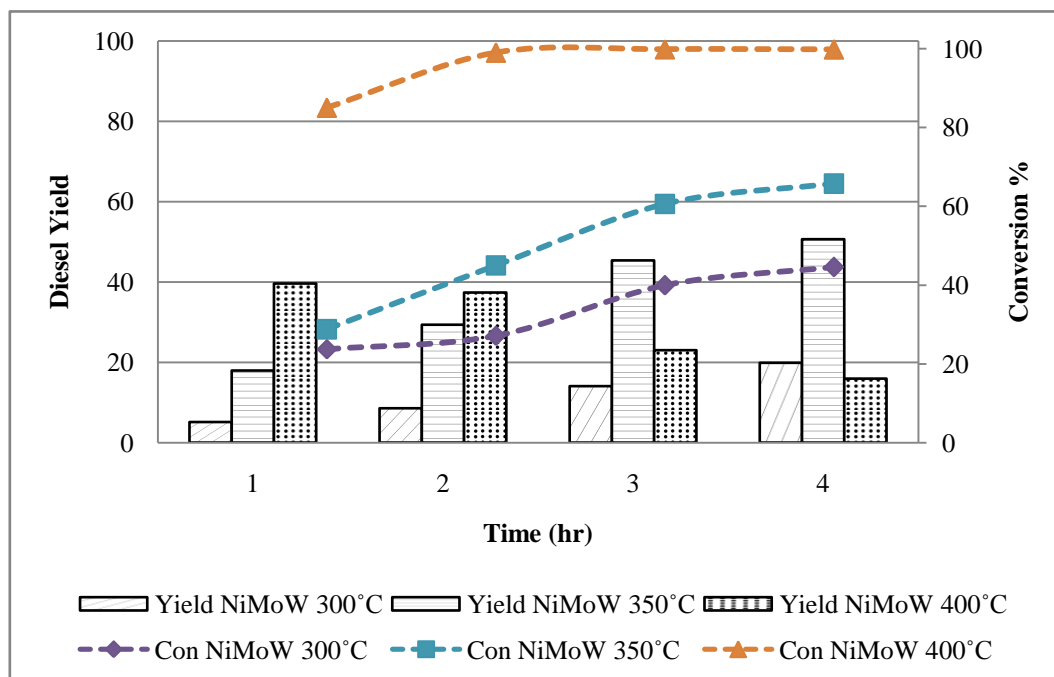


**Figure 5.18** Conversion of palmitic acid and diesel yield obtain from NiMoW/ $\gamma$ Al<sub>2</sub>O<sub>3</sub> catalyst under hydrogen pressure 40 bar

### 5.2.2 Effect of Catalysts to Ratio of $C_{n-1}/C_n$ Product

The results gathered in Table 5.1-5.3 Provide the ratio of the products from decarboxylation accompanied with decarbonylation ( $C_{n-1}$ ) to those from hydrodeoxygenation ( $C_n$ ). It was revealed that CoMo catalyst has higher in the product ratio, compared to CoMoW catalyst because the tungsten loading on CoMo catalyst was selective to hydrodeoxygenation path way, giving the products containing the even number of carbon atom higher than the odd number. Moreover, the opposite trend was found from the hydroprocessing process with CoMo catalyst. The selective pathway via decarboxylation and decarbonylation was proposed for the process with NiMoW.

**Table 5.3** Ratio  $C_{17}/C_{18}$  obtain from the hydroprocessing process fed by oleic acid

Catalysts	Reaction time (hr)			
	1	2	3	4
CoMo	2.7	3.15	3.40	2.98
CoMoW	1.68	1.79	1.67	1.9
NiMo	5.12	4.6	3.76	3.46
NiMoW	5.56	5.84	4.2	3.75

**Table 5.4** Ratio  $C_{17}/C_{18}$  obtain from the hydroprocessing process fed by Stearic acid

Catalysts	Reaction time (hr)			
	1	2	3	4
CoMo	3.59	2.59	4.32	4.22
CoMoW	2.6	2.31	3.4	2.98
NiMo	1.97	2.55	2.06	1.73
NiMoW	3.31	3.41	2.46	2.53

**Table 5.5** Ratio  $C_{15}/C_{16}$  obtain from the hydroprocessing process fed by palmitic acid

Catalysts	Reaction time (hr)			
	1	2	3	4
CoMo	2.84	2.84	3.15	2.76
CoMoW	2.09	2.45	2.35	2.14
NiMo	3.31	3.42	3.36	3.37
NiMoW	1.99	1.99	2.08	1.92

## CHAPTER VI

### CONCLUSIONS AND RECOMMENDATIONS

In this chapter presents the summation obtained from the experimental results and the recommendations of this research for the future study.

#### 6.1 Conclusions

According to the hydroprocessing process of fatty acid for biodiesel production, there are three main reactions composed of hydrodeoxygenation, decarboxylation and decarbonylation.

The process considering various fatty acid the maximum yield of 66.9% could be achieved from the oleic process operated with NiMoW catalyst at temperature of 350 °C and hydrogen pressure of 40 bar for 2 hours. It was found that it is suitable to give the maximum diesel range yield. The highest yields of diesel range operated with NiMo, CoMo and CoMoW were 47.48% 54.28% and 57.6% respectively.

For the addition of tungsten on the catalysts, it provides higher yield, compared to the operation with the absence of tungsten. Tungsten could enhance the hydrodeoxygenation reaction when tungsten was added to CoMo catalyst, whereas the reduction in the reduction in that reaction was presented in case of NiMoW catalyst. Tungsten increases the hydrodeoxygenation reaction when added to CoMo catalyst but it decreases hydrodeoxygenation reaction when added to NiMo catalyst.

## 6.2 Recommendations

1. The continuous flow in the lab scale instead of batch operation as studied in this work should be developed for more realistic.
2. Since the promising catalyst such as oxide catalyst could help reducing the step of carbidation before the operation before operation.
3. The gaseous product obtain from the hydroprocessing process should be further analyzed along with the consideration of liquid products.

## REFERENCES

- Absi-Halabi M, Stanislaus A, Al-Dolama K. 1998. Performance comparison of alumina-supported Ni-Mo, Ni-W and Ni-Mo-W catalysis in hydrotreating vacuum residue. *Fuel* 77:787-90
- Bezergianni S, Dimitriadis A, Sfetsas T, Kalogianni A. 2010. Hydrotreating of waste cooking oil for biodiesel production. Part II: Effect of temperature on hydrocarbon composition. *Bioresource Technology* 101:7658-60
- Bezergianni S, Kalogianni A. 2009. Hydrocracking of used cooking oil for biofuels production. *Bioresource Technology* 100:3927-32
- Bezergianni S, Kalogianni A, Dimitriadis A. 2012. Catalyst evaluation for waste cooking oil hydroprocessing. *Fuel* 93:638-41
- Bezergianni S, Kalogianni A, Vasalos IA. 2009. Hydrocracking of vacuum gas oil-vegetable oil mixtures for biofuels production. *Bioresource Technology* 100:3036-42
- da Rocha Filho GN, Brodzki D, Djéga-Mariadassou G. 1993. Formation of alkanes, alkylcycloalkanes and alkylbenzenes during the catalytic hydrocracking of vegetable oils. *Fuel* 72:543-9
- Donnis B, Egeberg R, Blom P, Knudsen K. 2009. Hydroprocessing of Bio-Oils and Oxygenates to Hydrocarbons. Understanding the Reaction Routes. *Top Catal* 52:229-40
- Furimsky E. 2003. Metal carbides and nitrides as potential catalysts for hydroprocessing. *Applied Catalysis A: General* 240:1-28
- Guzman A, Torres JE, Prada LP, Nuñez ML. 2010. Hydroprocessing of crude palm oil at pilot plant scale. *Catalysis Today* 156:38-43
- Huber GW, O'Connor P, Corma A. 2007. Processing biomass in conventional oil refineries: Production of high quality diesel by hydrotreating vegetable oils in heavy vacuum oil mixtures. *Applied Catalysis A: General* 329:120-9
- Huirache-Acuña R, Pawelec B, Rivera-Muñoz E, Nava R, Espino J, Fierro JLG. 2009. Comparison of the morphology and HDS activity of ternary Co-Mo-W catalysts supported on P-modified SBA-15 and SBA-16 substrates. *Applied Catalysis B: Environmental* 92:168-84
- Krár M, Kovács S, Kalló D, Hancsók J. 2010. Fuel purpose hydrotreating of sunflower oil on CoMo/Al<sub>2</sub>O<sub>3</sub> catalyst. *Bioresource Technology* 101:9287-93
- Mikulec J, Cvengroš J, Joríková L, Banič M, Kleinová A. 2010. Second generation diesel fuel from renewable sources. *Journal of Cleaner Production* 18:917-26
- Rojanapipatkul S, Jongsomjit B. 2008. Synthesis of cobalt on cobalt-aluminate via solvothermal method and its catalytic properties for carbon monoxide hydrogenation. *Catalysis Communications* 10:232-6
- Sajkowski DJ, Oyama ST. 1996. Catalytic hydrotreating by molybdenum carbide and nitride: unsupported Mo<sub>2</sub>N and Mo<sub>2</sub>CAI<sub>2</sub>O<sub>3</sub>. *Applied Catalysis A: General* 134:339-49
- Sankaranarayanan TM, Banu M, Pandurangan A, Sivasanker S. 2011. Hydroprocessing of sunflower oil-gas oil blends over sulfided Ni-Mo-Al-zeolite beta composites. *Bioresource Technology* 102:10717-23



- Santos PS, Santos HS, Toledo SP. 2000. Standard transition aluminas. Electron microscopy studies. *Materials Research* 3:104-14
- Schwartz V, Oyama ST, Chen JG. 2000. Supported Bimetallic Nb–Mo Carbide: Synthesis, Characterization, and Reactivity. *The Journal of Physical Chemistry B* 104:8800-6
- Sebos I, Matsoukas A, Apostolopoulos V, Papayannakos N. 2009. Catalytic hydroprocessing of cottonseed oil in petroleum diesel mixtures for production of renewable diesel. *Fuel* 88:145-9
- Sigurdson S, Sundaramurthy V, Dalai AK, Adjaye J. 2008. Phosphorus promoted trimetallic NiMoW/ $\gamma$ -Al<sub>2</sub>O<sub>3</sub> sulfide catalysts in gas oil hydrotreating. *Journal of Molecular Catalysis A: Chemical* 291:30-7
- Šimáček P, Kubička D. 2010. Hydrocracking of petroleum vacuum distillate containing rapeseed oil: Evaluation of diesel fuel. *Fuel* 89:1508-13
- Šimáček P, Kubička D, Šebor G, Pospíšil M. 2009. Hydroprocessed rapeseed oil as a source of hydrocarbon-based biodiesel. *Fuel* 88:456-60
- Šimáček P, Kubička D, Šebor G, Pospíšil M. 2010. Fuel properties of hydroprocessed rapeseed oil. *Fuel* 89:611-5
- Smejkal Q, Smejkalová L, Kubička D. 2009. Thermodynamic balance in reaction system of total vegetable oil hydrogenation. *Chemical Engineering Journal* 146:155-60
- Tailleur RG. 2006. Diesel upgrading into a low emissions fuel. *Fuel Processing Technology* 87:759-67
- Toba M, Abe Y, Kuramochi H, Osako M, Mochizuki T, Yoshimura Y. 2011. Hydrodeoxygenation of waste vegetable oil over sulfide catalysts. *Catalysis Today* 164:533-7
- Walendziewski J, Stolarski M, Łużny R, Klimek B. 2009. Hydroprocessing of light gas oil — rape oil mixtures. *Fuel Processing Technology* 90:686-91
- Yang XDE, (NJ, US). 2007. *United States*

## **APPENDICES**

## APPENDIX A

### CALCULATION OF CATALYST PREPARATION

#### 1. Preparation of 2.45wt% Ni 9.4wt% Mo/Al<sub>2</sub>O<sub>3</sub> is shown as follows:

Calculation for the preparation of nickel and molybdenum loading catalyst for

2.45Ni9.4Mo

Example calculation for the preparation of 2.45Ni9.4Mo/ $\gamma$ -Al<sub>2</sub>O<sub>3</sub>

Based on 100 g of catalyst used, the compositions of the catalyst are listed below:

$$\text{Ni} = 2.45 \text{ g}$$

$$\text{Mo} = 9.4 \text{ g}$$

$$\text{Al}_2\text{O}_3 = 100 - (2.45 + 9.4) = 88.15 \text{ g}$$

For 2 g of Al<sub>2</sub>O<sub>3</sub>,

$$\text{Weight of catalyst} = 2 \times (100/88.15) = 2.2689 \text{ g}$$

$$\text{Ni required} = 2.2689 \times (2.45/100)$$

$$= 0.0559 \text{ g}$$

Ni 0.0559 g was prepared from Ni(NO<sub>3</sub>)<sub>2</sub>·6H<sub>2</sub>O and molecular weight of Ni is 58.6934 g/mol.

$$\text{Ni(NO}_3)_2 \cdot 6\text{H}_2\text{O required} = ((M_w(\text{Ni(NO}_3)_2 \cdot 6\text{H}_2\text{O)}) / (M_w\text{Ni})) \times \text{Ni required}$$

$$= (290.79/58.6934) \times 0.0559 = 0.2932 \text{ g}$$

$$\text{Mo required} = 2.2689 \times (9.4/100) = 0.2133 \text{ g}$$

Mo 0.2133 g was prepared from  $(\text{NH}_4)_6\text{Mo}_7\text{O}_{24} \cdot 4\text{H}_2\text{O}$  and molecular weight of Mo is 95.94 g/mol

$$\begin{aligned} (\text{NH}_4)_6\text{Mo}_7\text{O}_{24} \cdot 4\text{H}_2\text{O} \text{ required} &= ((M_w((\text{NH}_4)_6\text{Mo}_7\text{O}_{24} \cdot 4\text{H}_2\text{O}) / (M_w\text{Mo})) \times \text{Mo required}) \\ &= (1234.58/95.94 \times 7) \times 0.2133 = 0.3924 \text{ g} \end{aligned}$$

2. Preparation of 2.54wt% Co 9.71%wt Mo/ $\gamma$ - $\text{Al}_2\text{O}_3$  is shown as follows:

Calculation for the preparation of cobalt and molybdenum loading catalyst for 2.54Co9.71Mo.

Example calculation for the preparation of 2.54Co9.71Mo/ $\gamma$ - $\text{Al}_2\text{O}_3$

Based on 100 g of catalyst used, the compositions of the catalyst are listed as follow:

$$\begin{aligned} \text{Co} &= 2.54 \text{ g} \\ \text{Mo} &= 9.71 \text{ g} \\ \text{Al}_2\text{O}_3 &= 100 - (2.54 + 9.71) = 87.75 \text{ g} \end{aligned}$$

For 2 g of  $\text{Al}_2\text{O}_3$

$$\text{Weight of catalyst} = 2 \times (100/87.75) = 2.2792 \text{ g}$$

$$\text{Co required} = 2.2689 \times (2.54/100) = 0.0579 \text{ g}$$

Co 0.0579 g was prepared from  $\text{Co}(\text{NO}_3)_2 \cdot 6\text{H}_2\text{O}$  and molecular weight of Co is 58.93 g/mol

$$\begin{aligned} \text{Co}(\text{NO}_3)_2 \cdot 6\text{H}_2\text{O} \text{ required} &= ((M_w(\text{Co}(\text{NO}_3)_2 \cdot 6\text{H}_2\text{O}) / (M_w\text{Co})) \times \text{Co required}) \\ &= (291.03/58.93) \times 0.0579 = 0.2859 \text{ g} \end{aligned}$$

$$\begin{aligned} \text{Mo required} &= 2.279 \times (9.71/100) \\ &= 0.2213 \text{ g} \end{aligned}$$

Mo 0.2213 g was prepared from  $(\text{NH}_4)_6\text{Mo}_7\text{O}_{24} \cdot 4\text{H}_2\text{O}$  and molecular weight of Mo is 95.94 g/mol

$$\begin{aligned} (\text{NH}_4)_6\text{Mo}_7\text{O}_{24} \cdot 4\text{H}_2\text{O} \text{ required} &= ((M_w((\text{NH}_4)_6\text{Mo}_7\text{O}_{24} \cdot 4\text{H}_2\text{O})) / (M_w\text{Mo})) \times \text{Mo required} \\ &= (1234.58/95.94 \times 7) \times 0.2213 = 0.4071 \text{ g} \end{aligned}$$

3. Preparation of 2.45wt% Ni 9.4wt% Mo 6%wt W/ $\gamma$ - $\text{Al}_2\text{O}_3$  is shown as follows:

Calculation for the preparation of nickel, molybdenum and tungsten loading catalyst for 2.45Ni 9.4Mo6W

Example calculation for the preparation of 2.45%Ni 9.4%Mo 6%W/ $\gamma$ - $\text{Al}_2\text{O}_3$

Based on 100 g of catalyst used, the compositions of the catalyst are list as follows:

$$\begin{aligned} \text{Ni} &= 2.45 \text{ g} \\ \text{Mo} &= 9.4 \text{ g} \\ \text{W} &= 6 \text{ g} \\ \text{Al}_2\text{O}_3 &= 100 - (2.45 + 9.4 + 6) = 82.15 \text{ g} \end{aligned}$$

For 2 g of  $\text{Al}_2\text{O}_3$

$$\text{Weight of catalyst} = 2 \times (100/82.15) = 2.4345 \text{ g}$$

$$\text{Ni required} = 2.4345 \times (2.45/100) = 0.0596 \text{ g}$$

Ni 0.0596 g was prepared from  $\text{Ni}(\text{NO}_3)_2 \cdot 6\text{H}_2\text{O}$  and molecular weight of Ni is 58.6934 g/mol

$$\begin{aligned} \text{Ni}(\text{NO}_3)_2 \cdot 6\text{H}_2\text{O} \text{ required} &= ((M_w(\text{Ni}(\text{NO}_3)_2 \cdot 6\text{H}_2\text{O})) / (M_w\text{Ni})) \times \text{Ni required} \\ &= (290.81/58.93) \times 0.0621 = 0.3066 \text{ g} \end{aligned}$$

$$\text{Mo required} = 2.4345 \times (9.4/100) = 0.2288 \text{ g}$$

Mo 0.2288 g was prepared from  $(\text{NH}_4)_6\text{Mo}_7\text{O}_{24} \cdot 4\text{H}_2\text{O}$  and molecular

weight of Mo is 95.94 g/mol

$$\begin{aligned} (\text{NH}_4)_6\text{Mo}_7\text{O}_{24} \cdot 4\text{H}_2\text{O} \text{ required} &= ((M_w((\text{NH}_4)_6\text{Mo}_7\text{O}_{24} \cdot 4\text{H}_2\text{O}) / (M_w\text{Mo})) \times \text{Mo required}) \\ &= (1234.58 / (95.94 \times 7)) \times 0.2288 = 0.4206 \text{ g} \end{aligned}$$

$$\text{W required} = 2.4345 \times (6/100) = 0.1460$$

W 0.1468 g was prepared from  $(\text{NH}_4)_{10}\text{W}_{12}\text{O}_{41} \cdot 7\text{H}_2\text{O}$  and molecular

weight of W is 183.84 g/mol

$$\begin{aligned} (\text{NH}_4)_{10}\text{W}_{12}\text{O}_{41} \cdot 7\text{H}_2\text{O} \text{ required} &= ((M_w((\text{NH}_4)_{10}\text{W}_{12}\text{O}_{41} \cdot 7\text{H}_2\text{O}) / (M_w\text{W})) \times \text{W required}) \\ &= (3168.66 \times 0.1460) / (183.84 \times 12) = 0.2096 \text{ g} \end{aligned}$$

4. Preparation of 2.54wt% Co 9.71wt% Mo 6wt%W/ $\gamma$ - $\text{Al}_2\text{O}_3$  is shown are listed as follows:

Calculation for the preparation of cobalt, molybdenum and tungsten loading catalyst for

2.54Co9.71Mo6W

Example calculation for the preparation of 2.54Co9.71Mo/ $\gamma$ -Al 2O3

Based on 100 g of catalyst used, the composition of the catalyst will be as follows:

$$\text{Co} = 2.54 \text{ g}$$

$$\text{Mo} = 9.71 \text{ g}$$

$$\text{W} = 6 \text{ g}$$

$$\text{Al}_2\text{O}_3 = 100 - (2.54 + 9.71 + 6) = 81.75 \text{ g}$$

For 2 g of  $\text{Al}_2\text{O}_3$

$$\text{Weight of catalyst} = 2 \times (100/81.75) = 2.4465 \text{ g}$$

$$\text{Co required} = 2.4465 \times (2.54/100) = 0.0621 \text{ g}$$

Co 0.0621 g was prepared from  $\text{Co}(\text{NO}_3)_2 \cdot 6\text{H}_2\text{O}$  and molecular weight of Co is 58.93 g/mol

$$\begin{aligned}\text{Co}(\text{NO}_3)_2 \cdot 6\text{H}_2\text{O} \text{ required} &= ((M_w(\text{Co}(\text{NO}_3)_2 \cdot 6\text{H}_2\text{O}) / (M_w\text{Co})) \times \text{Co required}) \\ &= (290.81/58.93) \times 0.0621 = 0.3066 \text{ g}\end{aligned}$$

$$\text{Mo required} = 2.4465 \times (9.71/100) = 0.2376 \text{ g}$$

Mo 0.2213 g was prepared from  $(\text{NH}_4)_6\text{Mo}_7\text{O}_{24} \cdot 4\text{H}_2\text{O}$  and molecular weight of Mo is 95.94 g/mol

$$\begin{aligned}(\text{NH}_4)_6\text{Mo}_7\text{O}_{24} \cdot 4\text{H}_2\text{O} \text{ required} &= ((M_w((\text{NH}_4)_6\text{Mo}_7\text{O}_{24} \cdot 4\text{H}_2\text{O}) / (M_w\text{Mo})) \times \text{Mo required}) \\ &= (1234.58/(95.94 \times 7)) \times 0.2376 = 0.4372 \text{ g}\end{aligned}$$

$$\text{W required} = 2.4465 \times (6/100) = 0.1468$$

W 0.1468 g was prepared from  $(\text{NH}_4)_{10}\text{W}_{12}\text{O}_{41} \cdot 7\text{H}_2\text{O}$  and molecular weight of W is 183.84 g/mol

$$\begin{aligned}(\text{NH}_4)_{10}\text{W}_{12}\text{O}_{41} \cdot 7\text{H}_2\text{O} \text{ required} &= ((M_w((\text{NH}_4)_{10}\text{W}_{12}\text{O}_{41} \cdot 7\text{H}_2\text{O}) / (M_w\text{W})) \times \text{W required}) \\ &= (3168.66 \times 0.1468) / (183.84 \times 12) = 0.2108 \text{ g}\end{aligned}$$

## APPENDIX B

### CALIBRATION CURVE

The mole composition of raw-materials used in the experiments i.e. oleic acid, stearic acid and palmitic acid, were analyzed by mean of gas chromatography (Shimasu -14B) equipped with DB-2887 capillary column and flame ionization detector (FID). The calibration curve of oleic acid, stearic acid and palmitic acid are illustrate in Figures B.1-B.3

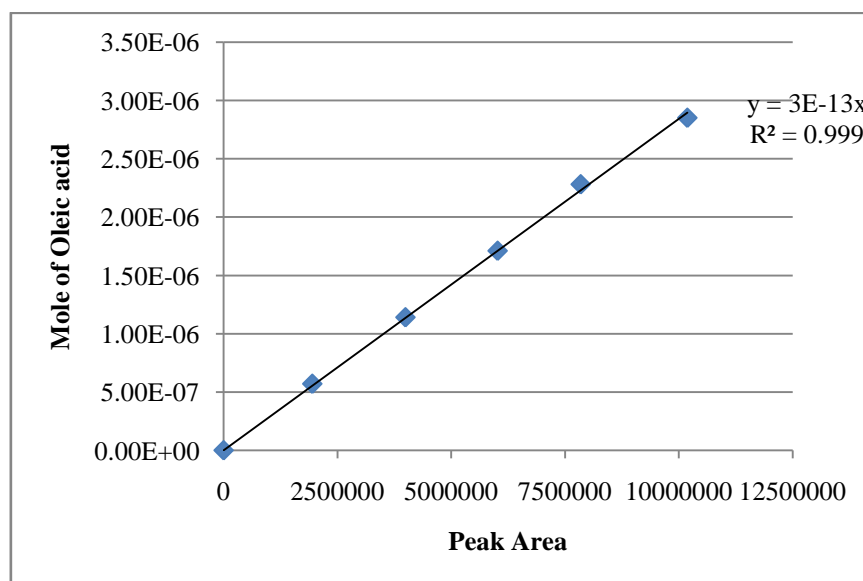


**Figure B.1** The calibration curve demonstrates the relationship between the composition and peak area of oleic acid.



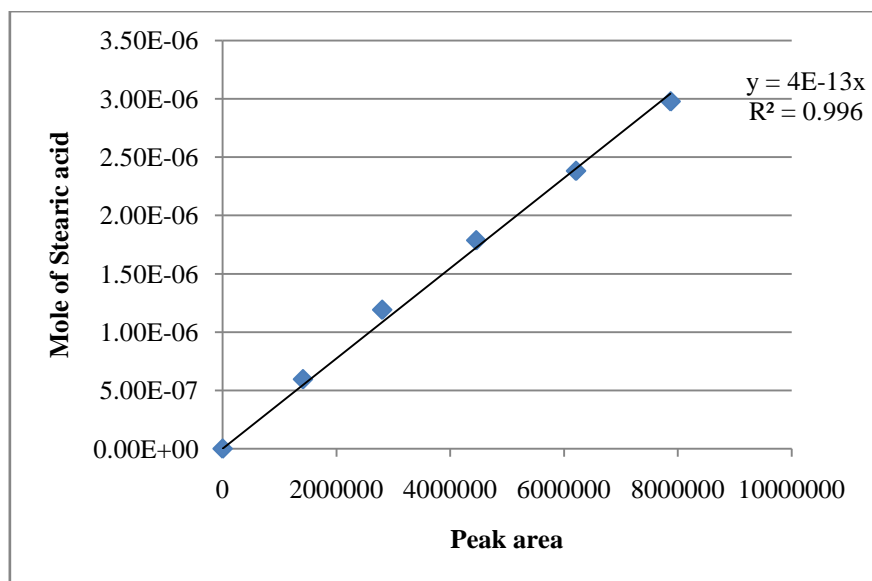


**Figure B.2** The calibration curve demonstrates the relationship between the composition and peak area of stearic acid

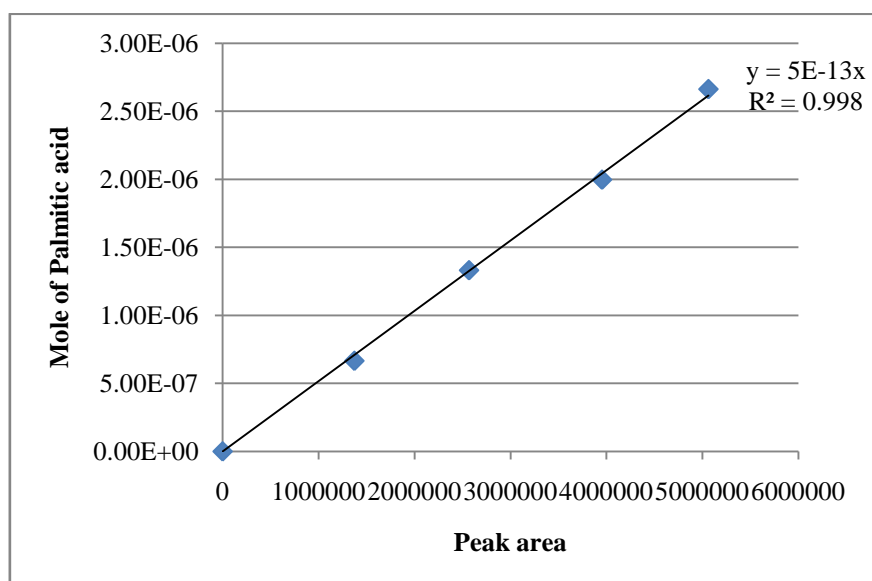


**Figure B.3** The calibration curve demonstrates the relationship between the composition and peak area of palmitic acid

**Table B.1** Operating conditions for gas chromatography.

Gas Chromatography	SHIMADZU GC-14B
Column	Capillary DB-2887
- Column material	Silica
- Length (m)	10
- Outer diameter (mm)	0.53
- Film thickness ( $\mu\text{m}$ )	3
-MaximumTemperature ( $^{\circ}\text{C}$ )	350
Carrier gas	He (99.999%)
Carrier gas flow (ml/min)	30
Column oven temperature program	
- initial column temperature ( $^{\circ}\text{C}$ )	40
- final column temperature ( $^{\circ}\text{C}$ )	330
Injector temperature ( $^{\circ}\text{C}$ )	250
Detector temperature ( $^{\circ}\text{C}$ )	340

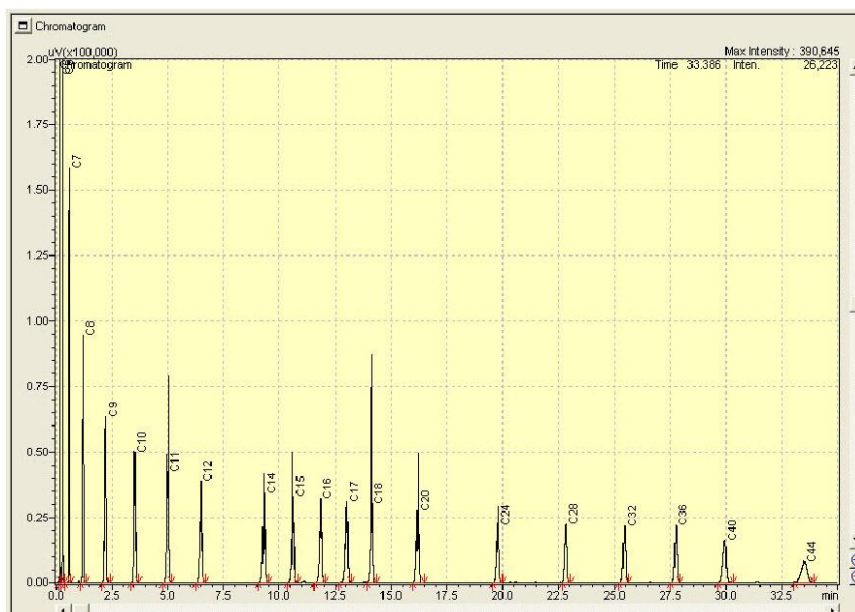


**Figure B.4** Chromatogram of calibration mixture reference.

In addition, the mixtures of C<sub>5</sub>-C<sub>44</sub> as listed in Table B.2 are considered as reference. Each component in the mixtures exhibits the peak with each retention time as displayed therefore hydrocarbons occurred in this research can be reference from this information.

**Table B.2** Results from chromatogram of calibration mixture reference.

Peak	Component	Rt (min)	Area	Conc.	Conc. (100%)	Units
1	C <sub>5</sub> H <sub>12</sub>	0.163	316798.1	0.9995	5.00033	%(w/w)
2	C <sub>6</sub> H <sub>14</sub>	0.3	345611.2	0.9995	5.00033	%(w/w)
3	C <sub>7</sub> H <sub>16</sub>	0.61	330865.1	0.9995	5.00033	%(w/w)
4	C <sub>8</sub> H <sub>18</sub>	1.22	63212.1	0.9995	5.00033	%(w/w)
5	C <sub>9</sub> H <sub>20</sub>	2.23	300457.4	0.9995	5.00033	%(w/w)
6	C <sub>10</sub> H <sub>22</sub>	3.55	291602.6	0.9995	5.00033	%(w/w)
7	C <sub>11</sub> H <sub>24</sub>	5.01	273183.5	0.9995	5.00033	%(w/w)

Peak	Component	Rt (min)	Area	Conc.	Conc. (100%)	Units
8	C <sub>12</sub> H <sub>26</sub>	6.5	262581.8	0.9995	5.00033	%(w/w)
9	C <sub>14</sub> H <sub>30</sub>	9.32	239842.9	0.9995	5.00033	%(w/w)
10	C <sub>15</sub> H <sub>32</sub>	10.62	233431.4	0.9995	5.00033	%(w/w)
11	C <sub>16</sub> H <sub>34</sub>	11.85	225150.5	0.9995	5.00033	%(w/w)
12	C <sub>17</sub> H <sub>36</sub>	13.02	216383.8	0.9995	5.00033	%(w/w)
13	C <sub>18</sub> H <sub>38</sub>	14.13	205113.8	0.9995	5.00033	%(w/w)
14	C <sub>20</sub> H <sub>42</sub>	16.19	187065.4	0.9995	5.00033	%(w/w)
15	C <sub>24</sub> H <sub>50</sub>	19.76	160614.5	0.9995	5.00033	%(w/w)
16	C <sub>28</sub> H <sub>58</sub>	22.83	160561.9	0.9995	5.00033	%(w/w)
17	C <sub>32</sub> H <sub>66</sub>	25.45	157273.7	0.9991	4.99832	%(w/w)
18	C <sub>36</sub> H <sub>74</sub>	27.76	153387.5	0.9995	5.00033	%(w/w)
19	C <sub>40</sub> H <sub>82</sub>	29.94	158740	0.9986	4.99582	%(w/w)
20	C <sub>44</sub> H <sub>90</sub>	33.52	146186.8	0.9995	5.00033	%(w/w)

## APPENDIX C

### CALCULATION OF ACID SITE

**Table C.1** Data for calculation of total acid sites

Catalysts	Area
NiMo/ $\gamma$ Al <sub>2</sub> O <sub>3</sub>	6.24624
CoMo/ $\gamma$ Al <sub>2</sub> O <sub>3</sub>	2.12358
NiMoW	2.64732
CoMoW	2.40624

#### Calculation of total acid sites

For CoMo/ $\gamma$ Al<sub>2</sub>O<sub>3</sub> catalyst, total acid site can be calculated from the following steps.

1. Calculation of peak volume from total peak area

From Figure C.1, the volume of NH<sub>3</sub> can be determined from equation  $y = 35.847x$ .

$$\begin{aligned} \text{The volume of NH}_3 &= 35.847 \times \text{area} \\ &= 35.847 \times 2.12358 = 76.1239 \text{ ml} \end{aligned}$$

2. Calculation of the adsorbed volume of 15% NH<sub>3</sub>

$$\begin{aligned} \text{The adsorbed volume of NH}_3 &= 0.15 \times \text{total peak volume} \\ &= 0.15 \times 76.1239 \text{ ml} = 11.4185 \text{ ml} \end{aligned}$$

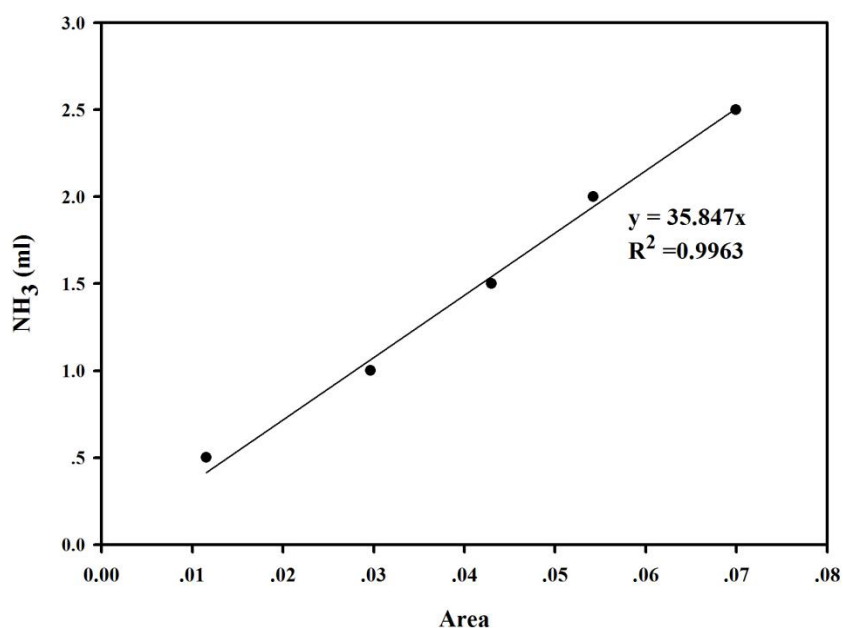


**Figure C.1** The calibration curve of ammonia.

3. The acid sites are calculated from the following equation

For CoMo/ $\gamma$ -Al<sub>2</sub>O<sub>3</sub>, 0.05000 g of this sample was measured, therefore

$$\text{The acid sites} = \frac{\text{Adsorbed volume (ml)} \times 101.325 \text{ Pa}}{8.314 \times 10^{-3} \frac{\text{Pa} \cdot \text{ml}}{\text{K} \cdot \mu\text{mol}} \times 298 \text{ K} \times \text{weight of catalyst (g)}}$$

$$\text{The acid sites} = \frac{11.4185 \times 101.325 \text{ Pa}}{8.314 \times 10^{-3} \frac{\text{Pa} \cdot \text{ml}}{\text{K} \cdot \mu\text{mol}} \times 298 \text{ K} \times 0.0500 \text{ g}}$$

$$= 9.33 \text{ mmol/g}$$

## APPENDIX D

## PRODUCTS DISTRIBUTION

## Stearic acid

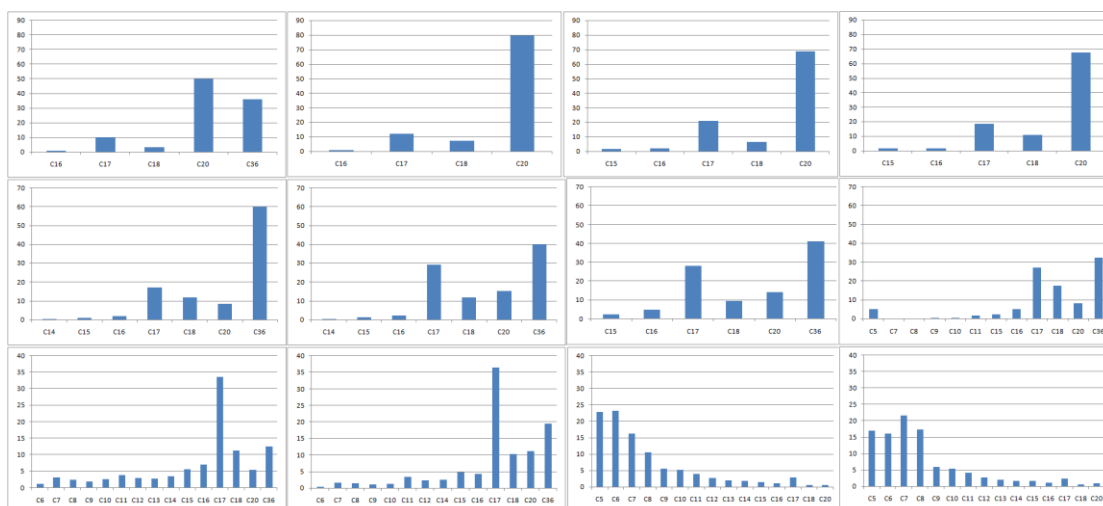


**Figure D.1** Product distribution of stearic acid obtain from CoMo/ $\gamma$ Al<sub>2</sub>O<sub>3</sub> catalyst under H<sub>2</sub> pressure of 40 bar

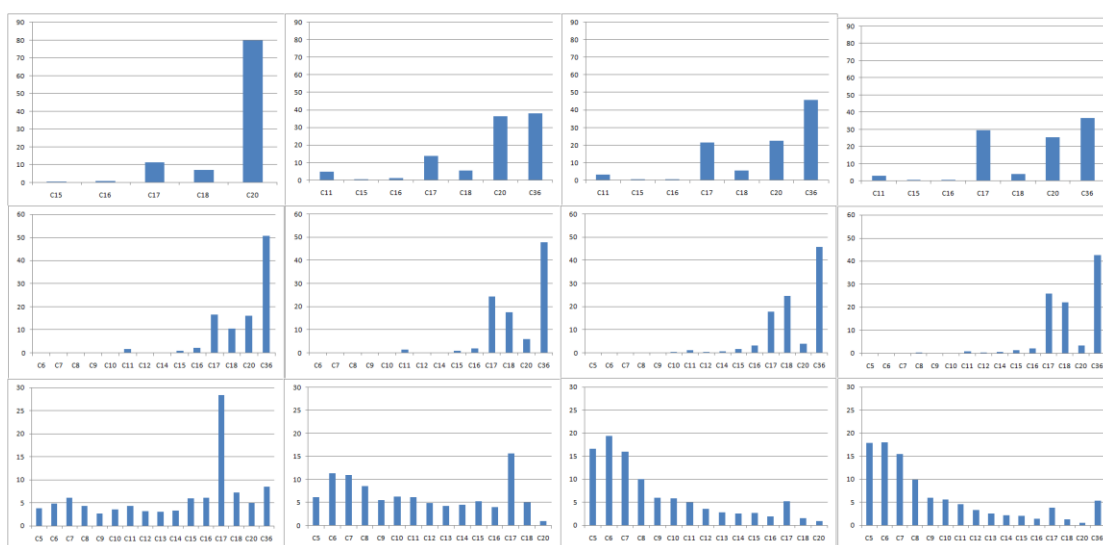


**Figure D.2** Product distribution of stearic acid obtain from CoMoW/ $\gamma$ Al<sub>2</sub>O<sub>3</sub> catalyst under H<sub>2</sub> pressure of 40 bar

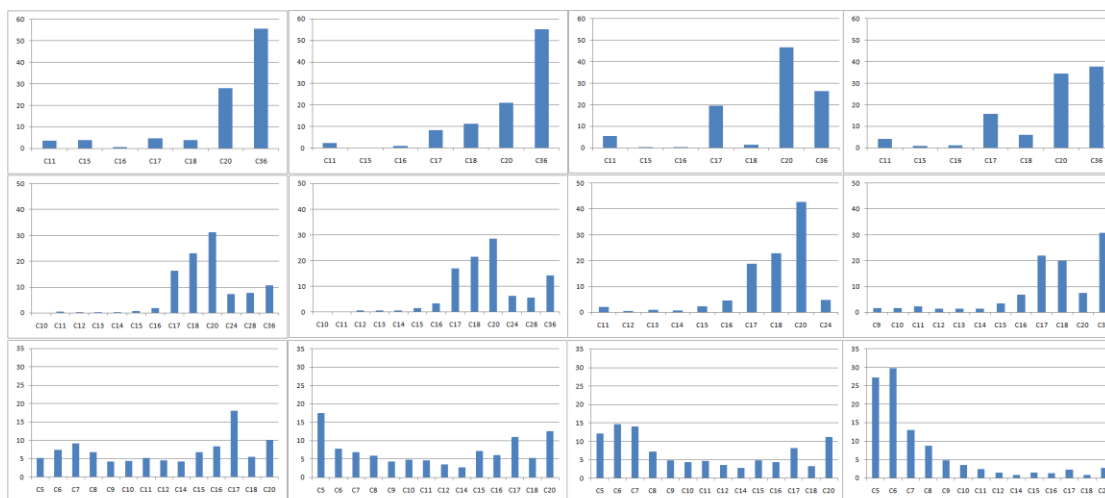


**Figure D.3** Product distribution of stearic acid obtain from NiMo/ $\gamma$ Al<sub>2</sub>O<sub>3</sub> catalyst under H<sub>2</sub> pressure of 40 bar

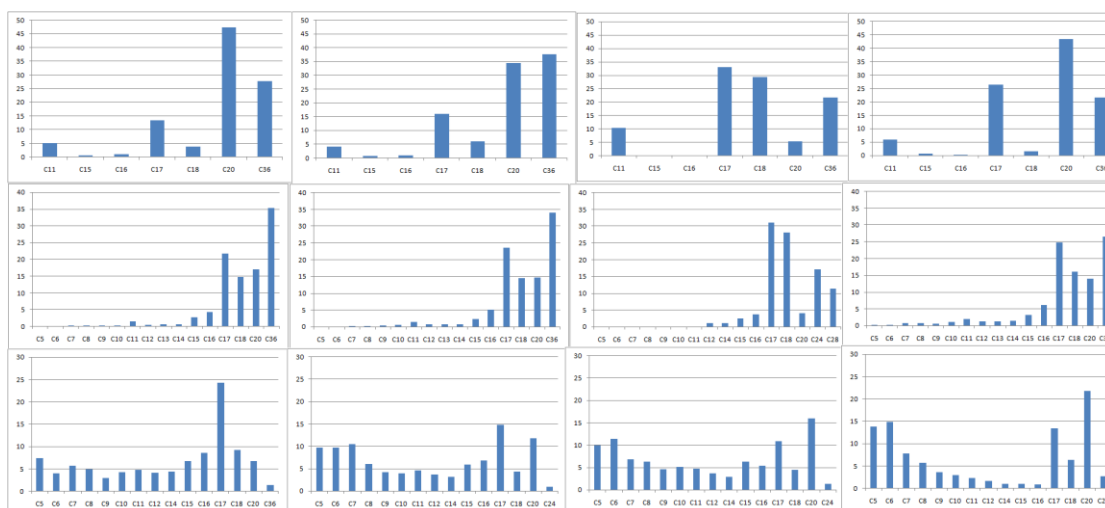


**Figure D.4** Product distribution of stearic acid obtain from NiMoW/ $\gamma$ Al<sub>2</sub>O<sub>3</sub> catalyst under H<sub>2</sub> pressure of 40 bar



### Palmitic acid

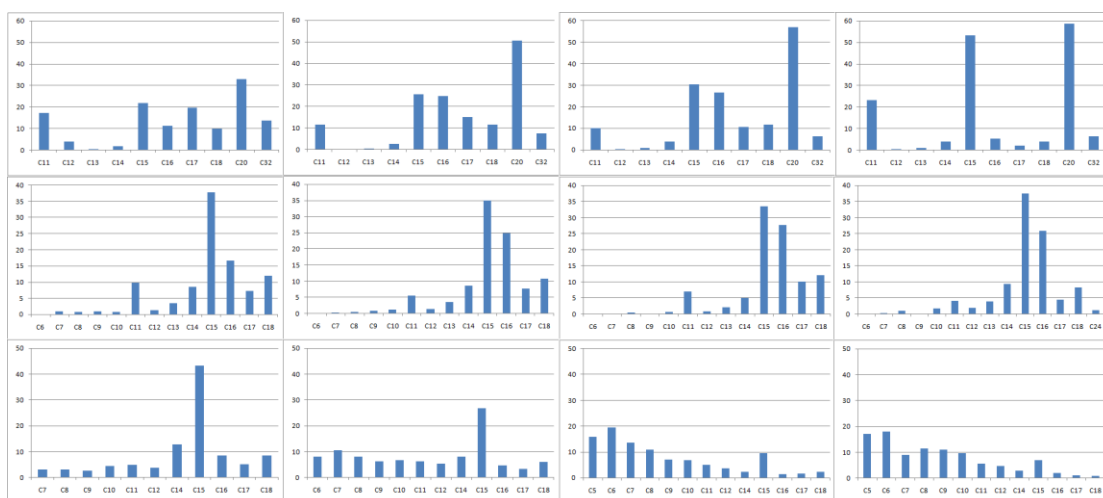


**Figure D.5** Product distribution of palmitic acid obtain from CoMo/ $\gamma$ Al<sub>2</sub>O<sub>3</sub> catalyst under H<sub>2</sub> pressure of 40 bar

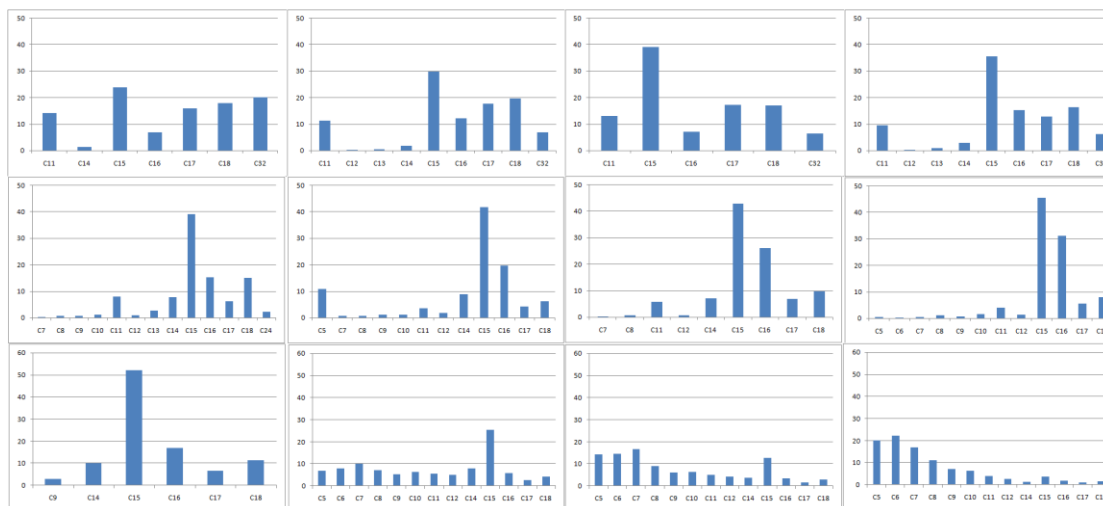


**Figure D.6** Product distribution of palmitic acid obtain from CoMoW/ $\gamma$ Al<sub>2</sub>O<sub>3</sub> catalyst under H<sub>2</sub> pressure of 40 bar

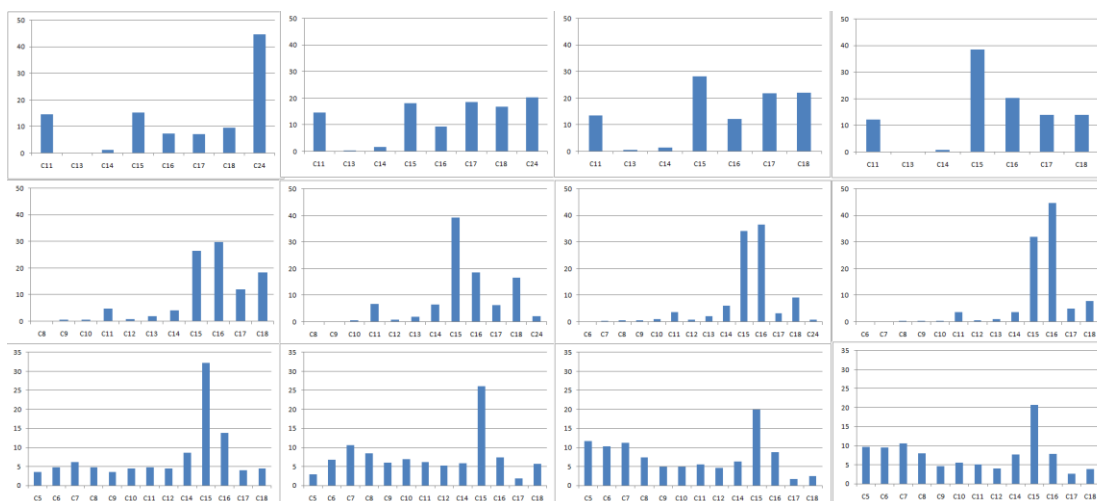


**Figure D.7** Product distribution of palmitic acid obtain from NiMo/ $\gamma$ Al<sub>2</sub>O<sub>3</sub> catalyst under H<sub>2</sub> pressure of 40 bar

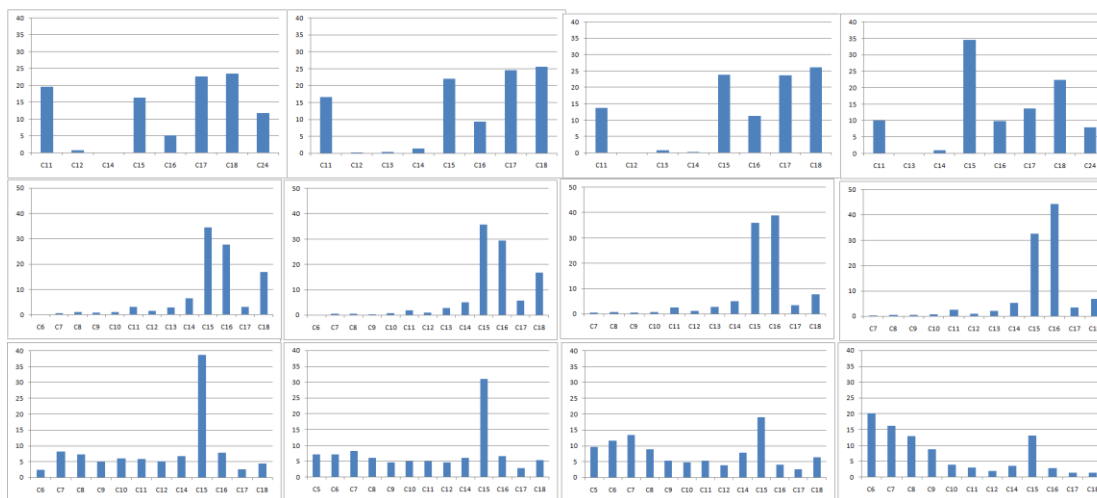


**Figure D.8** Product distribution of palmitic acid obtain from NiMoW/ $\gamma$ Al<sub>2</sub>O<sub>3</sub> catalyst under H<sub>2</sub> pressure of 40 bar

## APPENDIX E

### LIST OF PUBLICATION

Pongsatorn Jantharak, Worapon Kiatkittipong, Suwimol Wongsakulphasatch, Navadol Laosiripojana and Suttichai Assabumrungrat, “Green diesel production from hydrotreating of oleic acid over CoMo/ $\gamma$ -Al<sub>2</sub>O<sub>3</sub> and CoMoW/ $\gamma$ -Al<sub>2</sub>O<sub>3</sub> catalyst”, PROCEEDING 19<sup>th</sup> Regional Symposium on Chemical Engineering (RSCE2012) ,Bali ,Indonesia 7<sup>th</sup>-8<sup>th</sup> November 2012.

## VITA

Mr.Pongsatorn Jantharak was born in May 4<sup>th</sup> ,1988 in Songkhla, Thailand. His address is 11 Moo.10 Soi Kanchanawanich59 Kanchanawanich Rd. Tambon Khaorupchang MuangSongkhla Thailand. He finished high school from Mahavajiravudh School He received his Bachelor's Degree in Chemical Engineering from Silpakorn University Samchandra Palace campus Nakornpathom,Thailand in February 2010. Since May 2011, he continue studying his master degree of Chemical Engineering, Chulalongkorn University